

Room temperature phosphorescence and static excimer excitation of pyrene-modified (NCN) pincer bismuth complexes

Marcel Geppert, Michelle Müller, Michael Linseis, Rainer F. Winter*

^a Department of Chemistry, Universität Konstanz, 78467 Konstanz, Germany.

Supporting Information

Table of Contents

General	3
Synthesis	4
NMR Data	7
ESI-MS Data	11
Single Crystal X-ray Diffraction Data	14
UV/Vis Spectroscopy	26
TD-DFT Data	28
Photoluminescence Data	33
References	39

List of Figures

Figure S1. ¹ H-NMR spectrum of NCHN _{pyr}	7
Figure S2. ¹³ C-NMR spectrum of NCHN _{pyr}	7
Figure S3. ¹ H-NMR spectrum of 1	8
Figure S4. ¹³ C-NMR spectrum of 1	8
Figure S5. ¹ H-NMR spectrum of 2	9
Figure S6. ¹³ C-NMR spectrum of 2	9
Figure S7. Temperature-dependent ¹ H-NMR spectra of 2 in CD ₂ Cl ₂	10
Figure S8. ESI-MS of NCHN _{pyr} (black measured, blue simulated).	11
Figure S9. ESI-MS of complex 1 (black measured, blue simulated).	12
Figure S10. ESI-MS of complex 2 (black measured, blue simulated).	13
Figure S11. Packing diagrams of complex 1 viewed along (a) the a-axis, (b) the b-axis, and (c) the c-axis of the unit cell.	18
Figure S12. Packing diagrams of complex 2 viewed along (a) the a-axis and (b) the b-axis of the unit cell.	24
Figure S13. Packing diagrams of complex 2 viewed along the c-axis of the unit cell.	25
Figure S14. UV/Vis absorption spectra of 1 , 2 , and NCHN _{pyr} in CH ₂ Cl ₂	26
Figure S15. Top: Geometry-optimized structure of complex 1 . Middle: MO diagrams of relevant molecular orbitals involved in the individual TD-DFT computed electronic transitions along with the corresponding electron density difference maps. A loss of electron density is indicated in blue, a gain	

in red colour. Bottom: Comparison between the experimental (black line) and the TD-DFT computed (blue line) electronic absorption spectra. Individual electronic transitions are indicated as coloured bars.	28
Figure S16. Left: Geometry-optimized structure of complex 2 along with comparison between the experimental (black line) and the TD-DFT computed (blue line) electronic absorption spectra. Individual electronic transitions are indicated as coloured bars. Right: MO diagrams of relevant molecular orbitals involved in the individual TD-DFT computed electronic transitions along with the corresponding electron density difference maps. A loss of electron density is indicated in blue, a gain in red colour.....	29
Figure S17. PL data at 77 K in MeTHF of (a) 1 at $c = 1 \mu\text{M}$. (b) 2 at $c = 1 \mu\text{M}$. (c) 1 at $c = 10 \mu\text{M}$. (d) 2 at $c = 10 \mu\text{M}$. (e) 1 at $c = 100 \mu\text{M}$. (f) 2 at $c = 100 \mu\text{M}$. (g) 1 at $c = 1 \text{mM}$. (h) 2 at $c = 1 \text{mM}$. Absorption spectra are depicted as black, emission spectra as red and excitation spectra as blue lines.	33
Figure S18. PL data at r.t. in degassed CH_2Cl_2 of (a) 1 at $c = 1 \mu\text{M}$. (b) 2 at $c = 1 \mu\text{M}$. (c) 1 at $c = 10 \mu\text{M}$. (d) 2 at $c = 10 \mu\text{M}$. (e) 1 at $c = 100 \mu\text{M}$. (f) 2 at $c = 100 \mu\text{M}$. (g) 1 at $c = 1 \text{mM}$. (h) 2 at $c = 1 \text{mM}$. Absorption spectra are depicted as black, emission spectra as red and excitation spectra as blue lines.	34
Figure S19. Lifetime measurements of (a) the 397 nm emission of 1 at 77 K in MeTHF; (b) the 610 nm emission of 1 at 77 K in MeTHF; (c) the 403 nm emission of 1 in degassed CH_2Cl_2 at r.t....	36
Figure S20. Lifetime measurements of (a) the 393 nm emission of 2 at 77 K in MeTHF; (b) the 595 nm emission of 2 at 77 K in MeTHF.....	37
Figure S21. Lifetime measurements of (a) the 393 nm emission of 2 at r.t. in degassed CH_2Cl_2 ; (b) the 430 nm emission of 2 at r.t. in degassed CH_2Cl_2 ; (c) the 610 nm emission of 2 at r.t. in degassed CH_2Cl_2	38

List of Tables

Table S1. Crystal data and structure refinement for 1	14
Table S2. Bond Lengths [\AA] for 1	15
Table S3. Bond Angles [$^\circ$] for 1	16
Table S4. Torsion Angles [$^\circ$] for 1	17
Table S5. Crystal data and structure refinement for 2	19
Table S6. Bond Lengths [\AA] for 2	20
Table S7. Bond Angles [$^\circ$] for 2	21
Table S8. Torsion Angles [$^\circ$] for 2	22
Table S9. XYZ coordinates of the DFT-optimized structure of complex 1	30
Table S10. XYZ coordinates of the DFT-optimized structure of complex 2	31
Table S11. Photoluminescence and absorption data for complexes 1 and 2	35

General

All syntheses were performed under a nitrogen inert gas atmosphere and protection from light, using standard Schlenk techniques. No uncommon hazards are involved, apart from those concomitant with work under cryogenic conditions (-70 °C, cooling baths with *iso*-propanol and dry ice; appropriate protective gloves should be worn) and the use of *t*-BuLi (appropriate protective clothing should be worn; handling and storage should be carried out exclusively under inert gas condition; protection from water and moisture should be guaranteed at all times; suitable fire extinguishing agents should be held available when handling this highly flammable chemical). 1,3-Dibromo-7-(*tert*-butyl)-pyrene¹ and (N₃CN)BiCl₂² were prepared according to literature-known procedures.

NMR Spectroscopy: ¹H-NMR (400 MHz) and ¹³C{¹H}-NMR (101 MHz) spectra were recorded in CDCl₃ or CD₂Cl₂ at 300 K using a Bruker Avance III 400 spectrometer. NMR spectra were referenced to residual protonated solvent signals (¹H) or to the solvent signal itself (¹³C). The assignment of signals is based on 2D NMR spectra. **Mass Spectrometry:** Mass spectra were recorded in the positive ion mode on an ESI-calibrated LTQ Orbitrap Velos Spectrometer with the direct injection of acetonitrile solutions.

X-Ray Crystallography: A STOE IPDS-II image plate diffractometer equipped with a Mo-K α or Cu-K α radiation source was used. Data acquisition was conducted at 100 K. The program package X-Area was used for data processing. Either semiempirical or spherical absorption corrections were performed. The structures were solved and refined with SHELXT^{3, 4} and OLEX2.⁵ All non-hydrogen atoms were refined anisotropically. Crystallographic data for the structures **1** and **2** have been deposited with the Cambridge Crystallographic Data Centre as supplementary publication numbers CCDC 2377089 and 2377088.

DFT and TD-DFT calculations: The ground state electronic structures of the full models of complexes **1** and **2** were calculated by density functional theory (DFT) methods using the Gaussian 16 program packages.⁶ Geometry optimization followed by vibrational analysis was performed in solvent media. Solvent effects were described by the SMD variation of IEFPCM implemented in the Gaussian program package with standard parameters for dichloromethane.⁷ The fully relativistic small-core multiconfiguration Dirac Hartree-Fock-adjusted pseudopotentials and the corresponding optimized set of basis functions for Bi (ECP60MDF)⁸ and 6-31G(d) polarized double- ζ basis sets⁹ for the remaining atoms were employed together with the Perdew, Burke, Ernzerhof exchange and correlation functional (PBE0).^{10, 11} The GaussSum program package was used to analyze the results,¹² while the visualization of the results was performed with the Avogadro program package.¹³ Graphical representations of molecular orbitals were generated with the help of GNU Parallel¹⁴ and plotted using the vmd program package¹⁵ in combination with POV-Ray.¹⁶

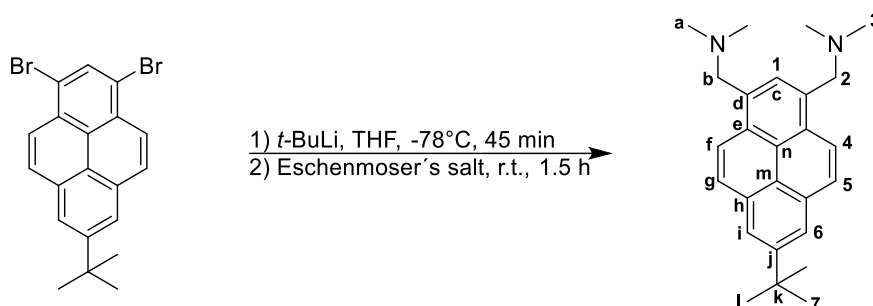
UV/Vis Spectroscopy: UV/Vis/NIR spectra of CH₂Cl₂ and MeTHF solutions of ligand NCHN_{pyr}, as well as complexes **1** and **2** were recorded on a TIDAS fiber optic diode array spectrometer (combined MCS UV/NIR and PGS NIR instrumentation) from J&M in HELMA quartz cuvettes with 1.0 cm optical path lengths.

Photoluminescence: Luminescence spectra and lifetimes of MeTHF and CH₂Cl₂ solutions of the respective compound were measured on a PicoQuant FluoTime 300 spectrometer. Absolute

quantum yields were determined with an integrating sphere within the FluoTime 300 spectrometer. Solutions were deaerated through three cycles of freeze-pump-thaw.

Synthesis

Ligand $NCHN_{\text{pyr}}$

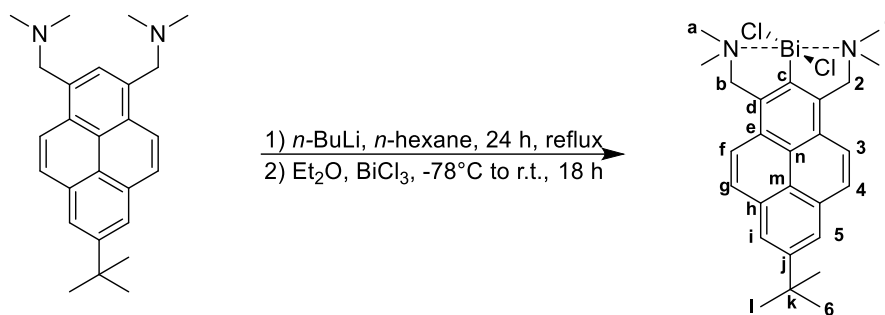


A solution of 1,3-dibromo-7-(*tert*-butyl)-pyrene¹ (2.00 g, 4.81 mmol, 1.00 eq) in 70 mL of THF was cooled to $-78\text{ }^{\circ}\text{C}$. 10.1 mL of a 1.9 M *n*-pentane solution of *t*-BuLi (19.2 mmol, 4.00 eq) was slowly added and the mixture was stirred for 45 min at $-78\text{ }^{\circ}\text{C}$. Then, Eschenmoser's salt (4.07 g, 22.00 mmol, 4.60 eq) was added and the reaction mixture was allowed to warm to r.t. and stirred for 90 min. THF was removed *in vacuo* and the reaction was quenched with water (50 mL). 50 mL of EtOAc were added and the phases were separated. The aqueous phase was extracted with EtOAc (3 x 25 mL), the organic phases were combined, dried over MgSO_4 , and the solvent was removed *in vacuo*. Impurities could be removed by column chromatography with CH_2Cl_2 as the eluent. The product remained on the top of the column and could be extracted from the silica gel with a $\text{CH}_2\text{Cl}_2/\text{NEt}_3$ solution (1:1). $NCHN_{\text{pyr}}$ was obtained as an orange solid (1.59 g, 4.27 mmol, 89% yield).

$^1\text{H-NMR}$ (CDCl_3 , 400 MHz) δ [ppm]: 8.49 (d, $^3J_{\text{HH}} = 9.1\text{ Hz}$, 2H, H^5), 8.26 (s, 2H, H^6), 8.11 (d, $^3J_{\text{HH}} = 9.4\text{ Hz}$, 2H, H^4), 7.91 (s, 1H, H^1), 4.10 (s, 4H, H^2), 2.38 (s, 12H, H^3), 1.63 (s, 9H, H^7).

$^{13}\text{C-NMR}$ (CDCl_3 , 101 MHz) δ [ppm]: 148.9 (C^j), 131.7 (C^h), 131.0 (C^d), 130.3 (C^c), 129.4 (C^e), 127.4 (C^f), 125.5 (C^n), 123.8 (C^g), 123.3 (C^m), 122.4 (C^i), 62.5 (C^b), 45.7 (C^a), 35.2 (C^k), 32.0 (C^l).

ESI-MS $\text{C}_{26}\text{H}_{32}\text{N}_2^+$, Calc. 372.2565, Found 372.2687, $\text{C}_{22}\text{H}_{24}\text{N}_2^+$, Calc. 316.1939, Found 316.2048, $\text{C}_{21}\text{H}_{19}^+$, Calc. 271.1481, Found 271.1484.



Synthesis and the purification were carried out under inert gas conditions. $NCHN_{\text{pyr}}$ (0.76 g, 1.54 mmol, 1.00 eq) was dissolved in 5 mL of *n*-hexane and *n*-BuLi (0.94 mL of a 1.6 M solution in *n*-hexane, 1.50 mmol, 1.00 eq) was added. The reaction mixture was heated to reflux for 24 h. Then, the solvent was removed *in vacuo*. The remaining solid was dissolved with 15 mL Et₂O and the resulting solution was slowly transferred by a cannula into a solution of BiCl₃ (0.48 g, 1.53 mmol, 1.00 eq) in 10 mL of Et₂O, which was precooled to -78 °C. After stirring for 1 h the reaction mixture was warmed to room temperature and stirred for 18 h. The solvent was removed *in vacuo*. The remaining solid was extracted with CH₂Cl₂. The insoluble solid was filtered off. Afterwards, the solution was stripped of the solvent *in vacuo*. The remaining solid was washed with *n*-hexane and then dried *in vacuo*. Complex **1** was obtained as a yellow-beige solid (244 mg, 0.38 mmol, 25%).

¹H-NMR (CD₂Cl₂, 400 MHz) δ [ppm]: 8.30 (s, 2H, H⁵), 8.22 (d, ³J_{HH} = 9.2 Hz, 2H, H³), 8.19 (d, ³J_{HH} = 9.2 Hz, 2H, H⁴), 5.32 (s, 4H, H²), 3.07 (s, 12H, H¹), 1.60 (s, 9H, H⁶).

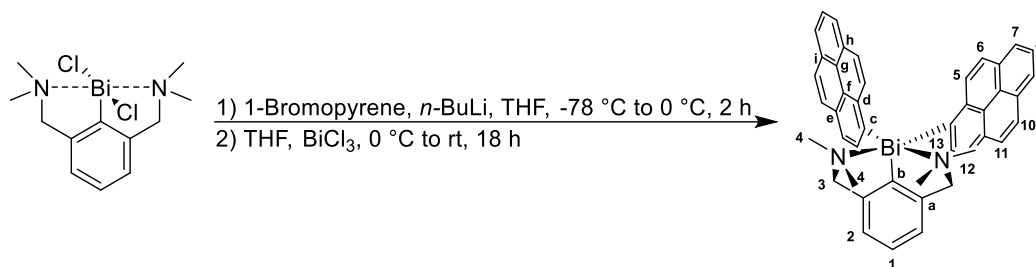
¹H-NMR (CDCl₃, 400 MHz) δ [ppm]: 8.25 (s, 2H, H⁵), 8.16 (m, 4H, H^{3,4}), 5.34 (s, 4H, H²), 3.10 (s, 12H, H¹), 1.59 (s, 9H, H⁶).

¹³C-NMR (CD₂Cl₂, 101 MHz) δ [ppm]: 207.3 (C^c), 150.3 (C^j), 144.0 (C^e), 132.2 (C^d), 131.1 (C^h), 129.6 (C^g), 125.6 (Cⁿ), 124.4 (C^f), 123.7 (Cⁱ), 123.6 (C^m), 66.1 (C^b), 48.2 (C^a), 35.6 (C^k), 32.0 (C^l).

¹³C-NMR (CDCl₃, 101 MHz) δ [ppm]: 207.1 (C^c), 149.9 (C^j), 143.5 (C^e), 132.1 (C^d), 131.0 (C^h), 129.6 (C^g), 125.6 (Cⁿ), 124.0 (C^f), 123.5 (C^{i,m}), 66.0 (C^b), 48.1 (C^a), 35.4 (C^k), 32.0 (C^l).

ESI-MS BiC₂₆H₃₁N₂Cl⁺, Calc. 615.1974, Found 615.2006, Bi₂C₅₂H₆₂N₄Cl₃⁺, Calc. 1265.3642, Found 1265.3714.

The sample for combustion analysis was obtained by extracting the solid into 25 mL of benzene, filtering, and drying *in vacuo* to yield the compound as benzene monosolvate. **Elemental analysis** Calc. for C₂₆H₃₁BiCl₂N₂×C₆H₆: C, 52.68; H, 5.11; N, 3.84. Found: C, 52.60; H, 5.47; N, 3.64.



Synthesis and the purification were carried out under inert gas conditions. 1-Bromopyrene (280 mg, 1.00 mmol, 2.00 eq) was dissolved in 5 mL of dry THF and the solution was cooled to -78 °C. A 2.5 M solution of *n*-BuLi (0.499 mL, 1.25 mmol, 2.50 eq) in hexane was added dropwisely. The orange reaction mixture was stirred for 2 h and warmed to 0 °C. (N₂CN)BiCl₂ (235 mg, 0.500 mmol, 1.00 eq) was suspended in 20 mL of dry THF and the suspension was cooled to 0 °C. The lithiated species was added dropwisely to the suspension. The yellow reaction mixture was stirred for 1 h at 0 °C and for 18 h at room temperature. The solvent was removed *in vacuo*. The solid was washed with 20 mL of *n*-hexane and 90 mL of acetonitrile and then dried *in vacuo*. The remaining solid was extracted with benzene. The solution was filtered and the solvent was evaporated to yield **2** as a beige solid (208 mg, 0.26 mmol, 52%).

¹H-NMR (CD₂Cl₂, 400 MHz) δ [ppm] = 8.99 (d, 2H, H¹⁰, ³J_{HH} = 7.6 Hz), 8.82 (d, 2H, H⁹, ³J_{HH} = 9.2 Hz), 8.10-8.03 (m, 6H, H^{7-8,10-13}), 7.96 (d, 2H, H¹¹, ³J_{HH} = 7.6 Hz), 7.90-7.85 (m, 6H, H^{7-8,10-13}), 7.40 (t, 1H, H¹, ³J_{HH} = 6.6 Hz), 7.32 (d, 2H, H², ³J_{HH} = 7.3 Hz), 3.32 (s, 4H, H³), 1.73 (s, 12H, H⁴).

¹³C-NMR (CD₂Cl₂, 101 MHz) δ [ppm]: 166.2, 149.8, 137.5, 136.6, 132.2, 131.8, 131.5, 130.2, 129.9, 128.7, 128.2, 128.1, 126.9, 126.8, 126.7, 125.9, 125.7, 125.6, 124.7, 124.6, 67.5, 44.8.

ESI-MS BiC₂₈H₂₈N₂⁺, Calc. 601.2051, Found 601.2030.

Elemental analysis Calc. for C₄₄H₃₇BiN₂: C, 64.83; H, 4.65; N, 3.49. Found: C, 64.89; H, 4.86; N, 3.36.

NMR Data

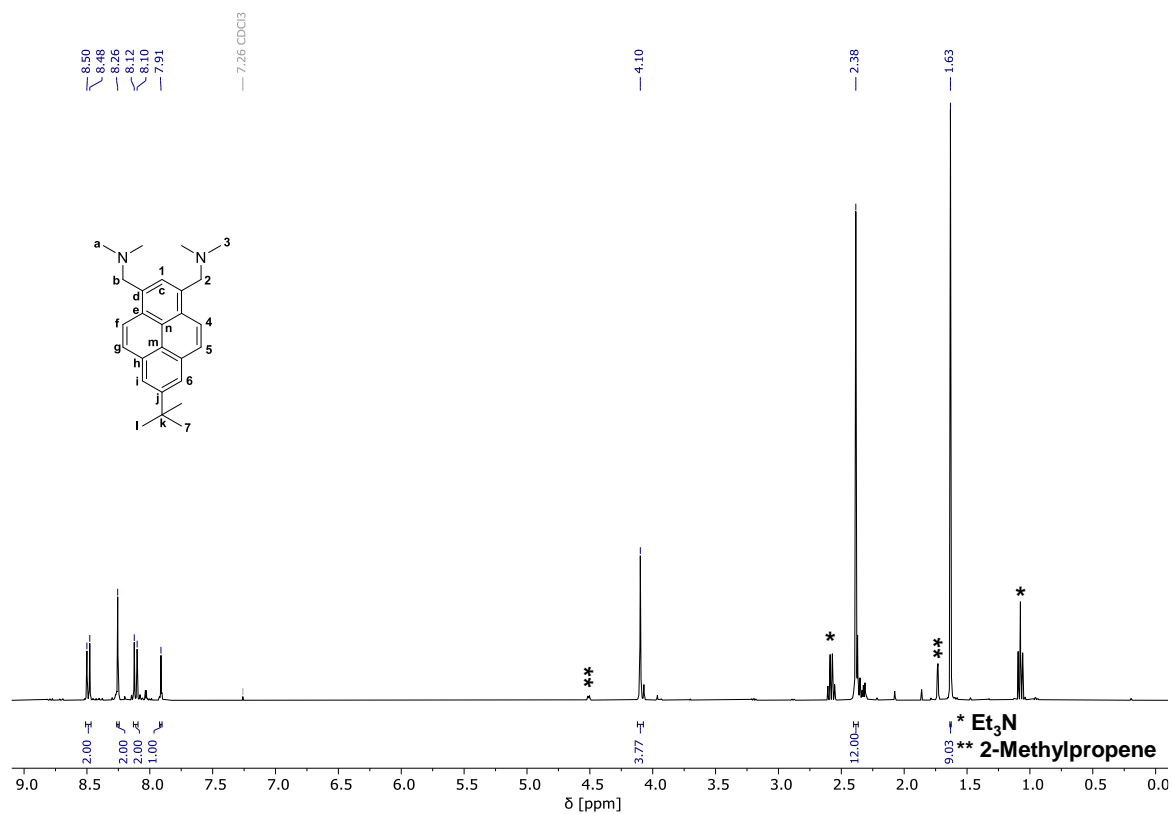


Figure S1. ¹H-NMR spectrum of *NCHN*_{pyr}.

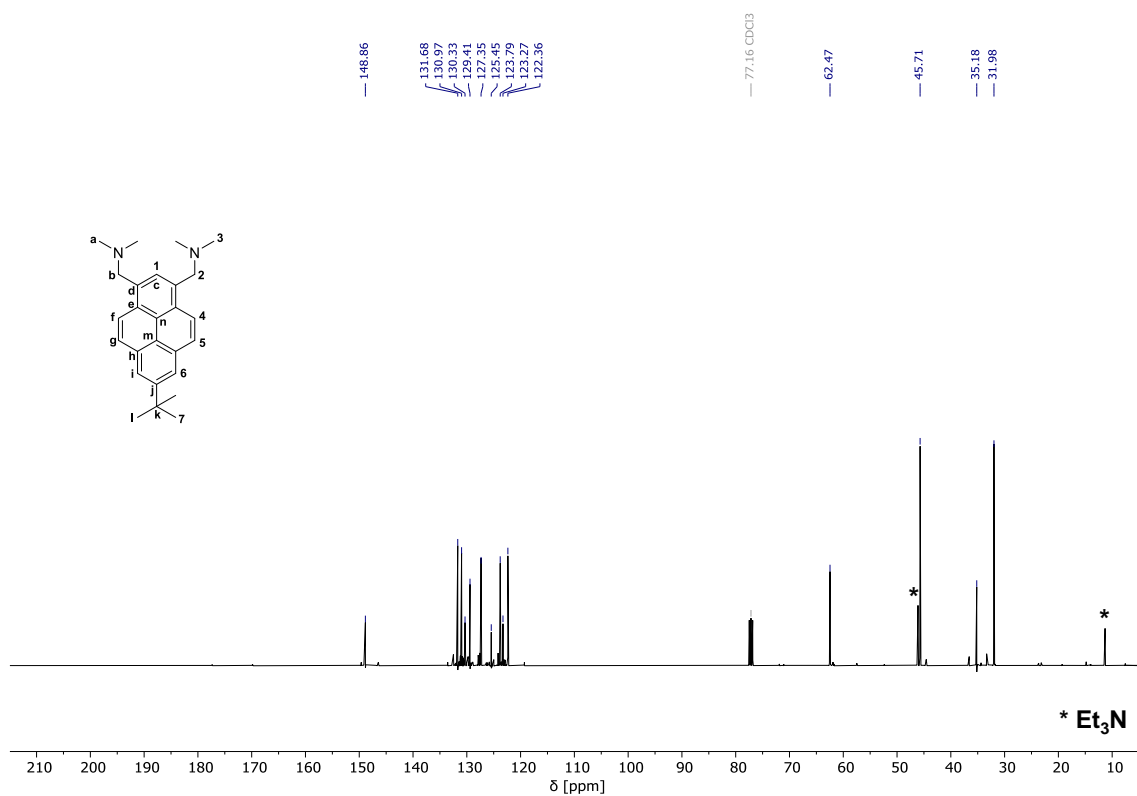


Figure S2. ¹³C-NMR spectrum of *NCHN*_{pyr}.

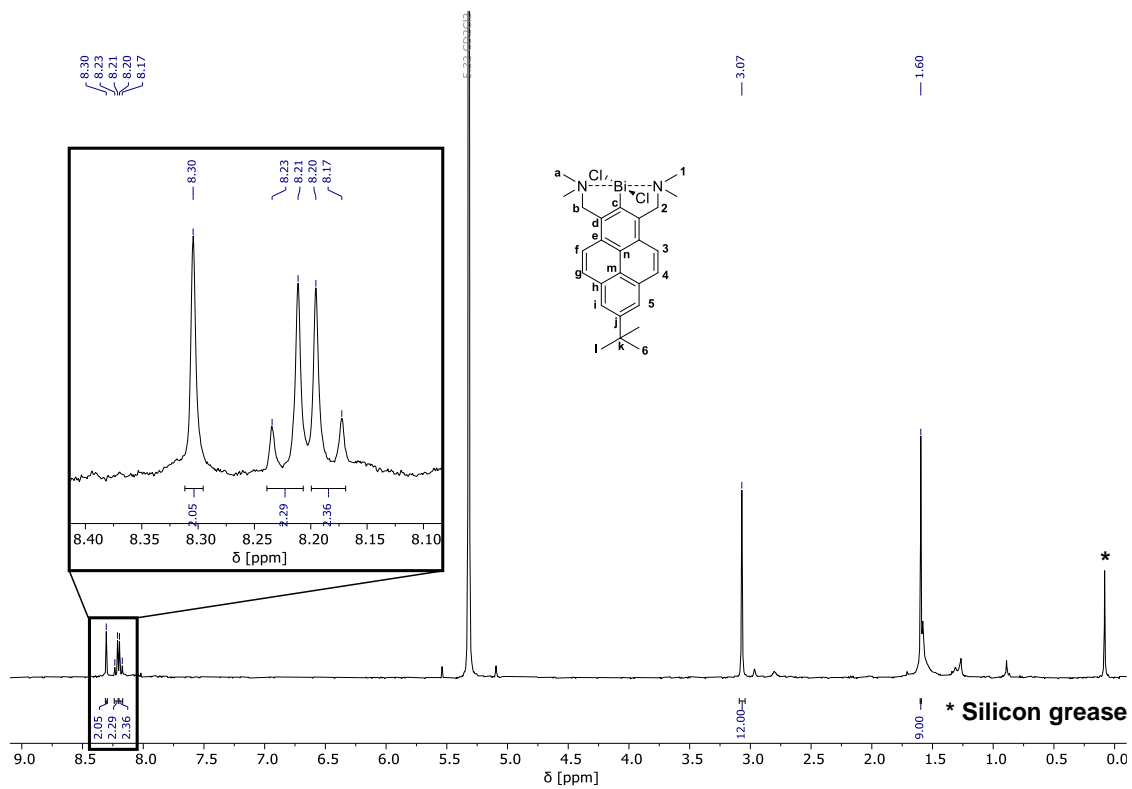


Figure S3. ¹H-NMR spectrum of **1**.

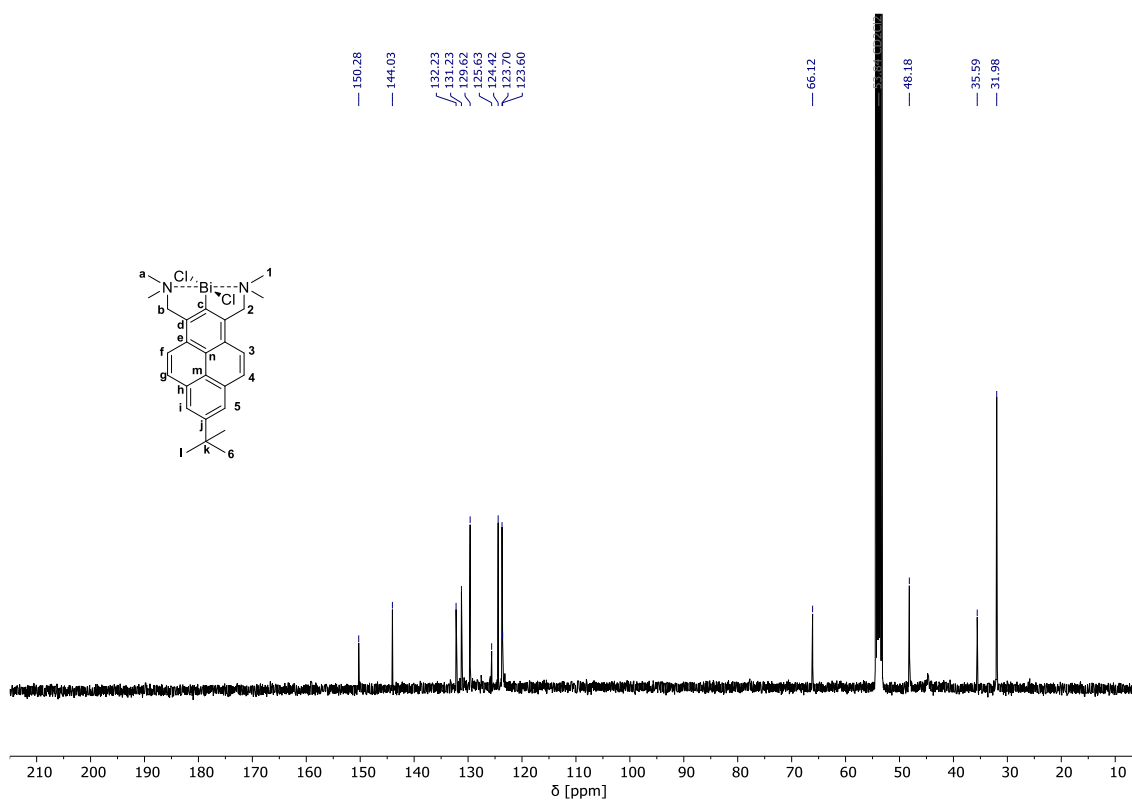


Figure S4. ¹³C-NMR spectrum of **1**.

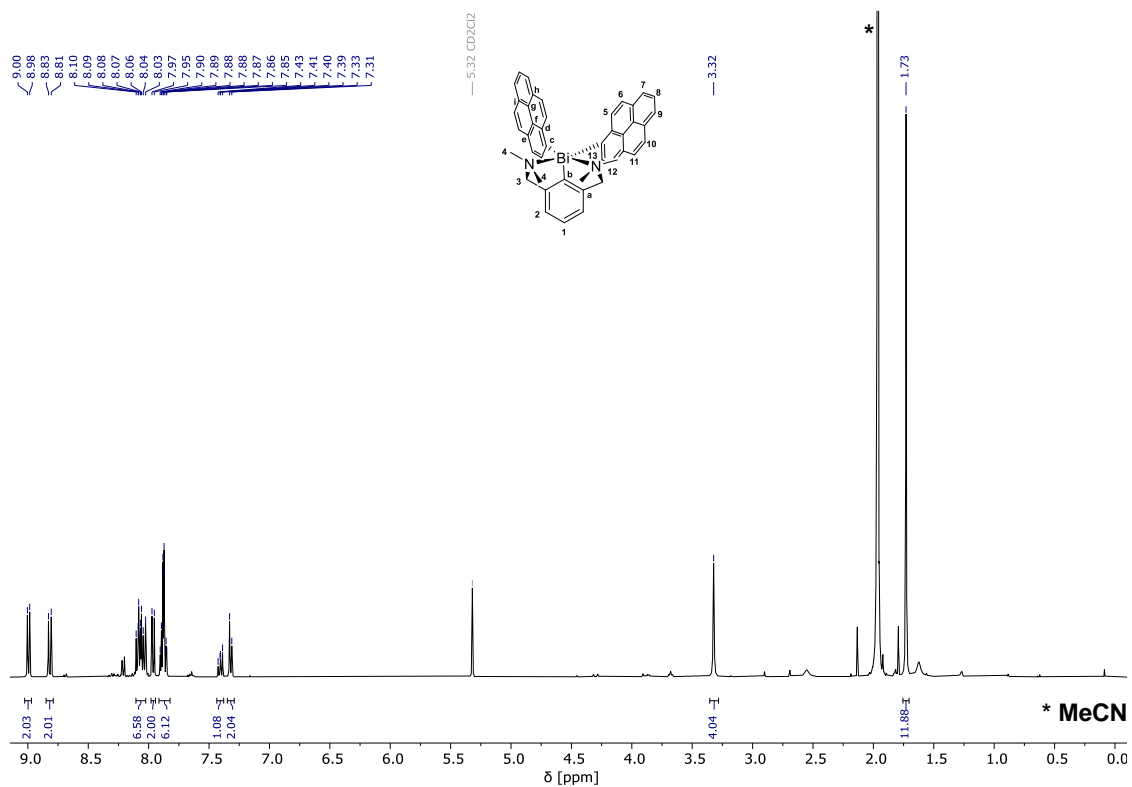


Figure S5. $^1\text{H-NMR}$ spectrum of 2.

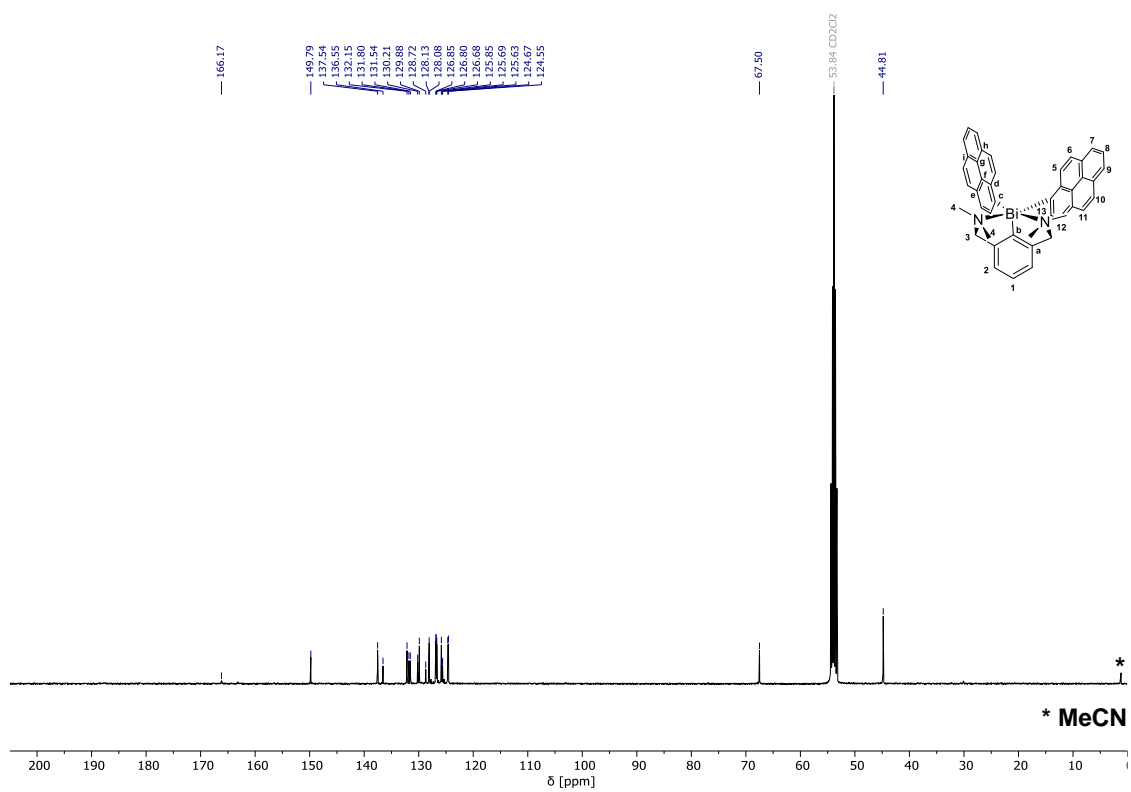


Figure S6. $^{13}\text{C-NMR}$ spectrum of 2.

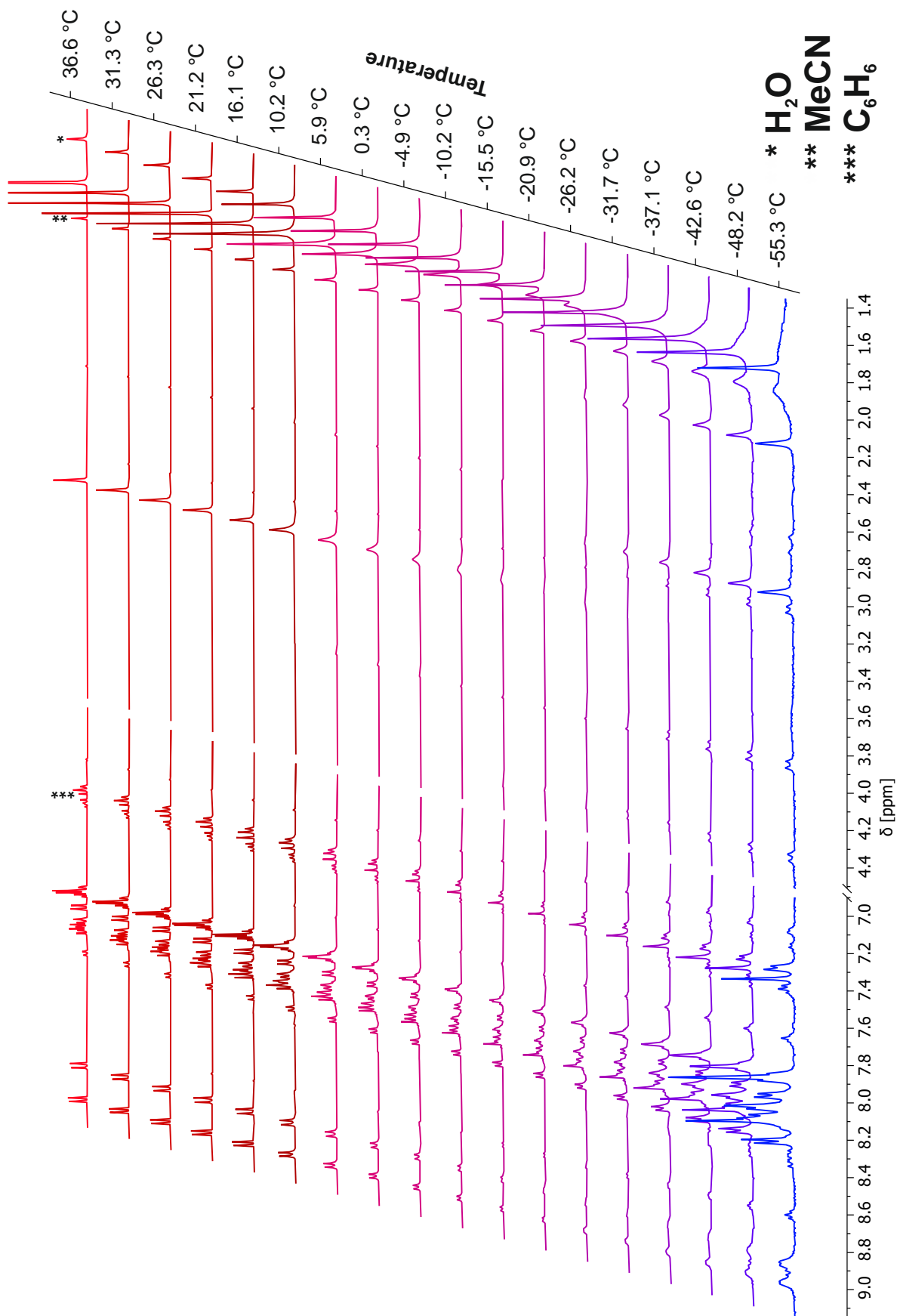
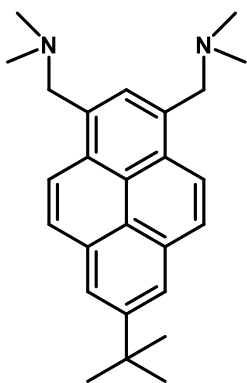
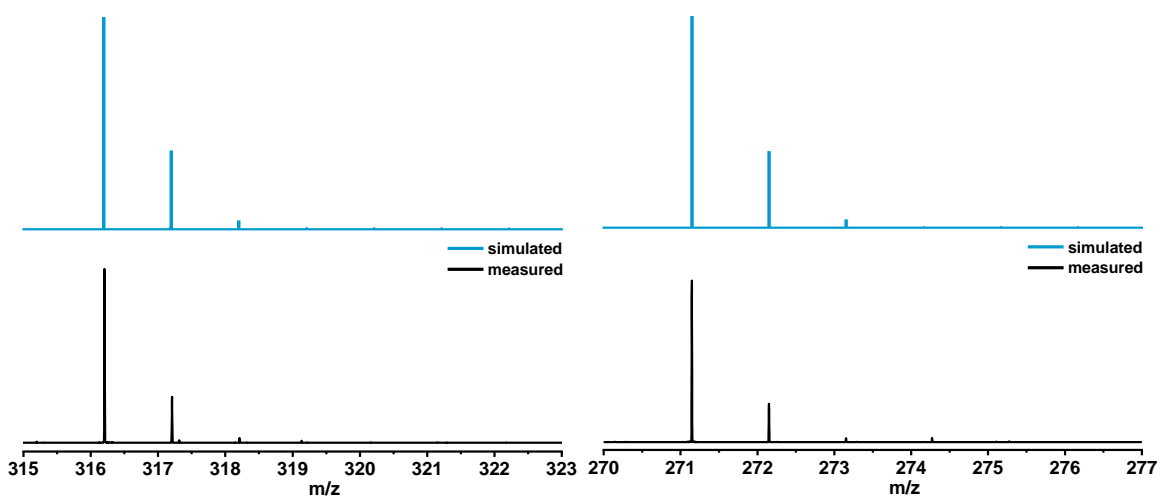
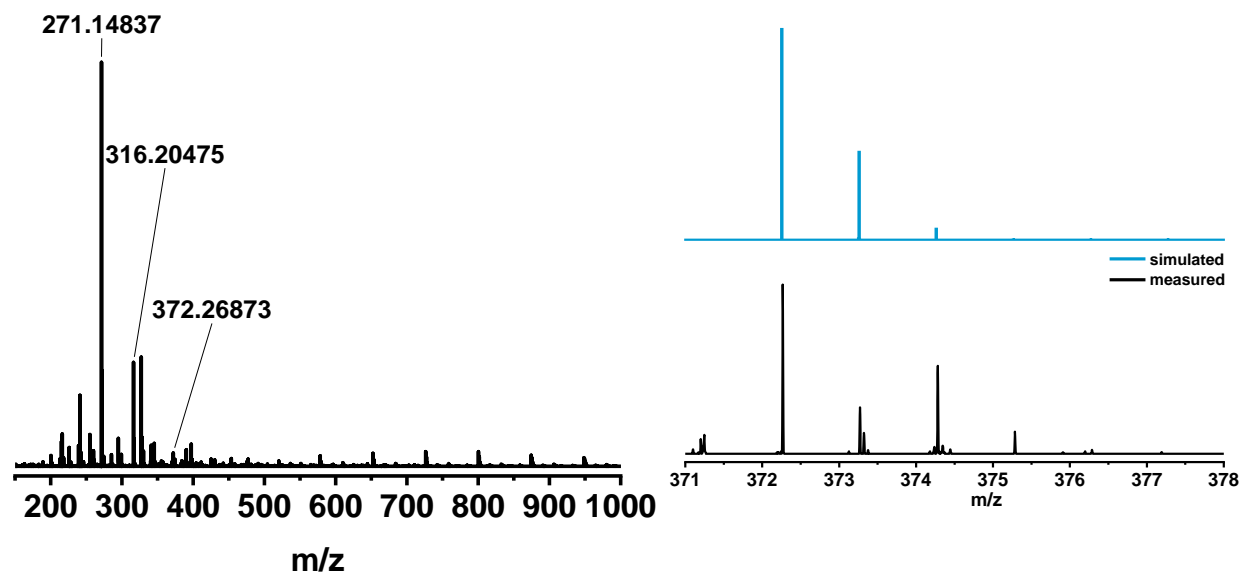
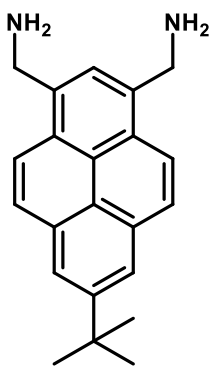


Figure S7. Temperature-dependent $^1\text{H-NMR}$ spectra of **2** in CD_2Cl_2 .

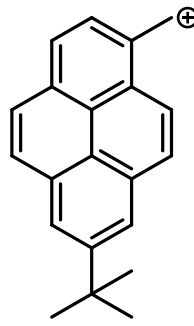
ESI-MS Data



Chemical Formula: $C_{26}H_{32}N_2$
Exact Mass: 372.2565

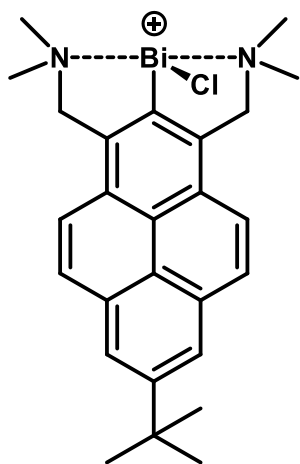
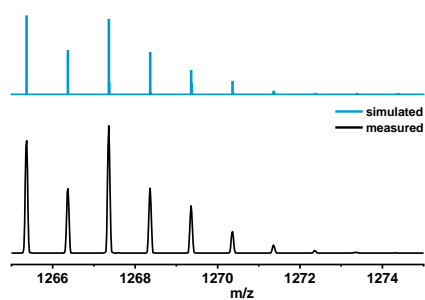
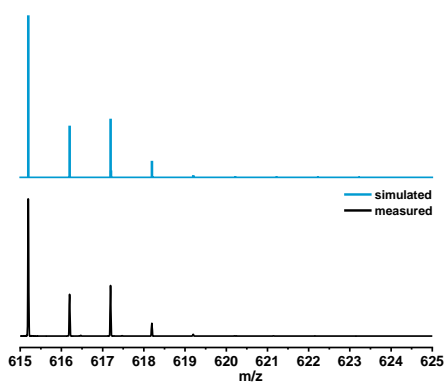
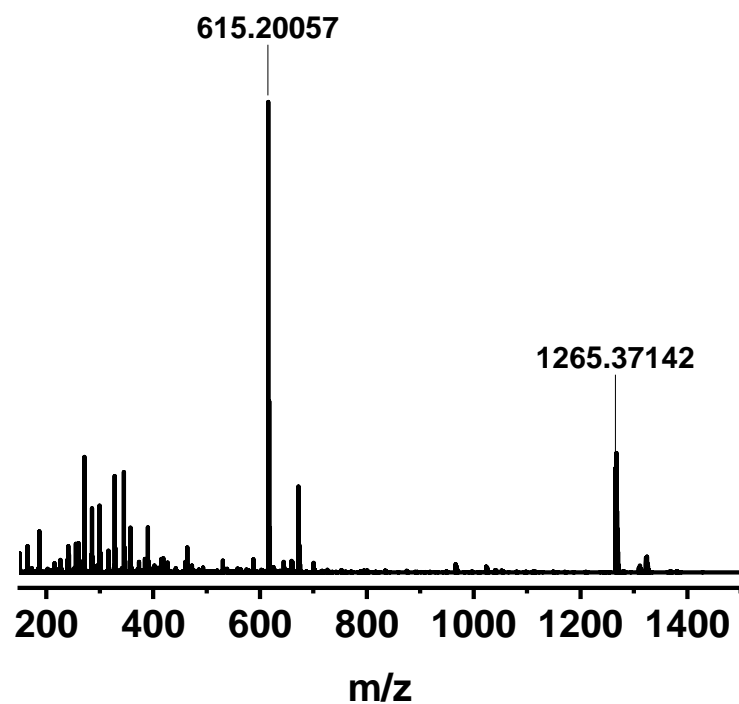


Chemical Formula: $C_{22}H_{24}N_2$
Exact Mass: 316.1939

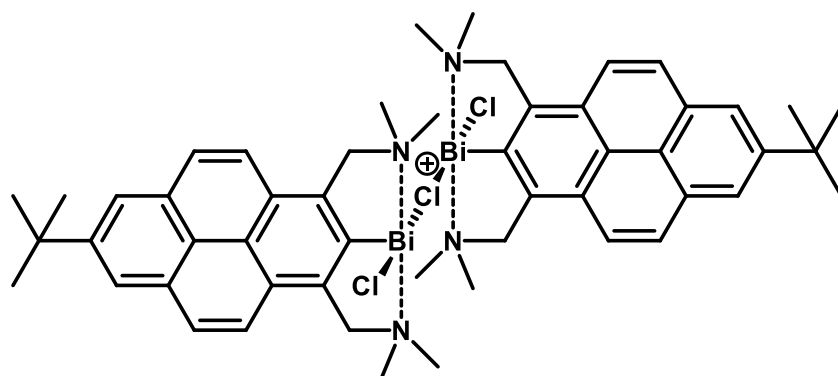


Chemical Formula: $C_{21}H_{19}^+$
Exact Mass: 271.1481

Figure S8. ESI-MS of $NCHN_{pyr}$ (black measured, blue simulated).

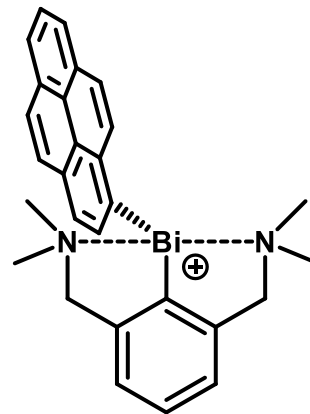
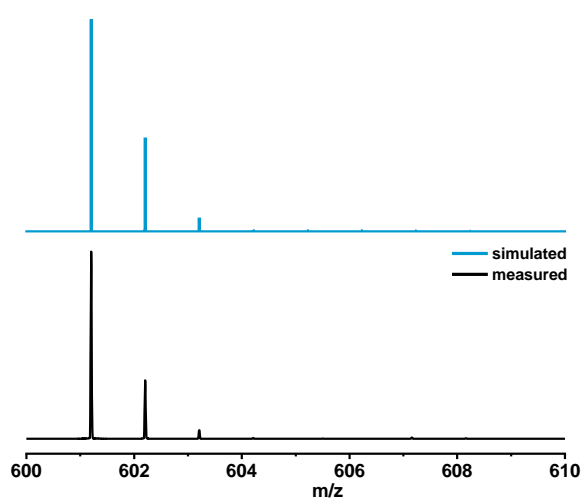
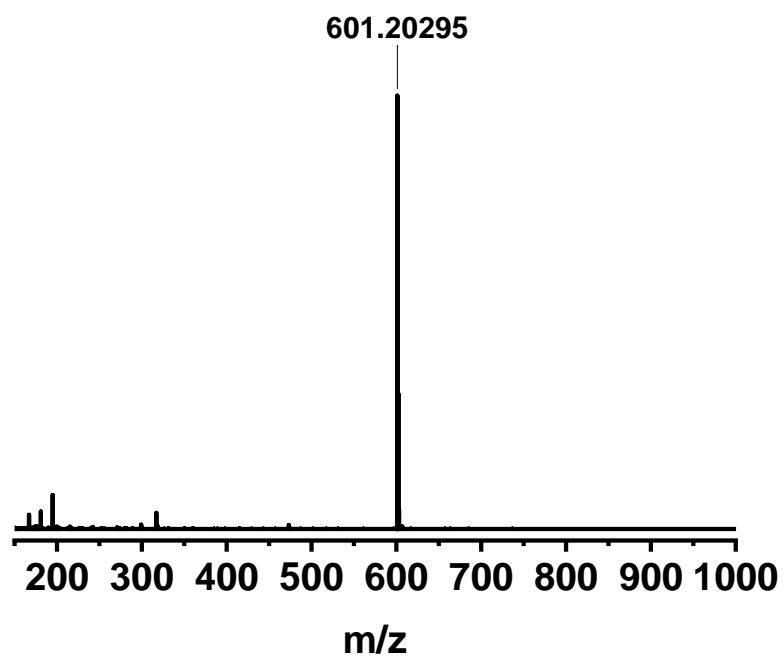


Chemical Formula: $C_{26}H_{31}BiClN_2^+$
Exact Mass: 615.1974



Chemical Formula: $C_{52}H_{62}Bi_2Cl_3N_4^+$
Exact Mass: 1265.3642

Figure S9. ESI-MS of complex **1** (black measured, blue simulated).



Chemical Formula: $\text{C}_{28}\text{H}_{28}\text{BiN}_2^+$
Exact Mass: 601.2051

Figure S10. ESI-MS of complex 2 (black measured, blue simulated).

Single Crystal X-ray Diffraction Data

Table S1. Crystal data and structure refinement for **1**.

Identification code	1
Empirical formula	$C_{31}H_{43}BiCl_2N_2$
Formula weight	723.55
Temperature/K	100
Crystal system	triclinic
Space group	$P\bar{1}$
$a/\text{\AA}$	8.0167(3)
$b/\text{\AA}$	13.3464(5)
$c/\text{\AA}$	15.4903(6)
$\alpha/^\circ$	113.090(3)
$\beta/^\circ$	92.143(3)
$\gamma/^\circ$	98.505(3)
Volume/ \AA^3	1499.52(10)
Z	2
$\rho_{\text{calc}}/\text{g/cm}^3$	1.602
μ/mm^{-1}	6.079
$F(000)$	720.0
Crystal size/ mm^3	$0.15 \times 0.1 \times 0.05$
Radiation	Mo $K\alpha$ ($\lambda = 0.71073$)
2Θ range for data collection/ $^\circ$	3.438 to 55.104
Index ranges	$-10 \leq h \leq 10, -17 \leq k \leq 17, -20 \leq l \leq 20$
Reflections collected	13209
Independent reflections	6856 [$R_{\text{int}} = 0.0477, R_{\text{sigma}} = 0.0600$]
Data/restraints/parameters	6856/0/334
Goodness-of-fit on F^2	1.140
Final R indexes [$I \geq 2\sigma(I)$]	$R_1 = 0.0558, wR_2 = 0.1191$
Final R indexes [all data]	$R_1 = 0.0827, wR_2 = 0.1456$
Largest diff. peak/hole / $e \text{\AA}^{-3}$	3.43/-2.98

Table S2. Bond Lengths [Å] for **1**.

Atom	Atom	Length/Å	Atom	Atom	Length/Å
Bi1	C11	2.726(2)	C4	C16	1.436(14)
Bi1	C12	2.660(3)	C4	C3	1.427(13)
Bi1	N1	2.489(9)	C4	C5	1.413(13)
Bi1	N2	2.519(8)	C21	C19	1.393(14)
Bi1	C1	2.235(10)	C6	C5	1.414(13)
N1	C9	1.472(13)	C20	C18	1.399(14)
N1	C8	1.478(14)	C16	C18	1.416(13)
N1	C7	1.508(14)	C16	C19	1.418(14)
N2	C12	1.466(12)	C3	C2	1.403(14)
N2	C11	1.483(13)	C3	C13	1.439(14)
N2	C10	1.484(12)	C18	C15	1.433(14)
C1	C6	1.403(13)	C19	C17	1.435(13)
C1	C2	1.374(14)	C5	C14	1.439(13)
C22	C23	1.534(13)	C15	C13	1.345(14)
C22	C21	1.420(13)	C14	C17	1.357(14)
C22	C20	1.363(14)	C2	C7	1.534(14)
C23	C26	1.550(15)	C29	C30	1.504(16)
C23	C24	1.522(14)	C29	C28	1.525(15)
C23	C25	1.510(14)	C30	C31	1.505(16)

Table S3. Bond Angles [°] for **1**.

Atom	Atom	Atom	Angle/°	Atom	Atom	Atom	Angle/°
C12	Bi1	C11	175.32(8)	C3	C4	C16	118.9(9)
N1	Bi1	C11	97.4(2)	C5	C4	C16	119.7(9)
N1	Bi1	C12	82.6(2)	C5	C4	C3	121.4(9)
N1	Bi1	N2	143.9(3)	C19	C21	C22	121.4(9)
N2	Bi1	C11	82.18(19)	C1	C6	C10	118.7(9)
N2	Bi1	C12	95.05(19)	C1	C6	C5	118.7(9)
C1	Bi1	C11	86.2(3)	C5	C6	C10	122.6(9)
C1	Bi1	C12	89.4(3)	C22	C20	C18	123.1(9)
C1	Bi1	N1	72.1(3)	C18	C16	C4	121.0(9)
C1	Bi1	N2	71.8(3)	C18	C16	C19	118.7(9)
C9	N1	Bi1	115.7(6)	C19	C16	C4	120.3(8)
C9	N1	C8	109.8(8)	C4	C3	C13	118.5(9)
C9	N1	C7	108.0(8)	C2	C3	C4	117.5(9)
C8	N1	Bi1	108.0(6)	C2	C3	C13	123.9(9)
C8	N1	C7	108.6(9)	C20	C18	C16	119.3(9)
C7	N1	Bi1	106.6(7)	C20	C18	C15	122.6(9)
C12	N2	Bi1	113.6(6)	C16	C18	C15	118.1(9)
C12	N2	C11	109.3(8)	C21	C19	C16	119.7(9)
C12	N2	C10	109.7(8)	C21	C19	C17	121.9(9)
C11	N2	Bi1	109.6(6)	C16	C19	C17	118.4(9)
C11	N2	C10	109.1(8)	C4	C5	C6	119.2(9)
C10	N2	Bi1	105.3(5)	C4	C5	C14	118.9(9)
C6	C1	Bi1	117.9(7)	C6	C5	C14	121.9(9)
C2	C1	Bi1	119.8(7)	C13	C15	C18	121.7(9)
C2	C1	C6	122.0(9)	C17	C14	C5	121.2(9)
C21	C22	C23	117.3(9)	C1	C2	C3	121.2(9)
C20	C22	C23	124.9(9)	C1	C2	C7	117.8(9)
C20	C22	C21	117.8(9)	C3	C2	C7	121.0(10)
C22	C23	C26	109.2(8)	C15	C13	C3	121.7(10)
C24	C23	C22	110.8(8)	C14	C17	C19	121.5(9)
C24	C23	C26	107.6(9)	C30	C29	C28	113.6(9)

Table S4. Torsion Angles [°] for **1**.

A	B	C	D	Angle/°	A	B	C	D	Angle/°
Bi1	N1	C7	C2	39.9(10)	C6	C1	C2	C7	-179.5(10)
Bi1	N2	C10	C6	39.2(9)	C6	C5	C14	C17	178.0(10)
Bi1	C1	C6	C10	-5.3(12)	C20	C22	C23	C26	119.2(11)
Bi1	C1	C6	C5	172.4(7)	C20	C22	C23	C24	-122.5(11)
Bi1	C1	C2	C3	-173.7(8)	C20	C22	C23	C25	-0.4(15)
Bi1	C1	C2	C7	6.6(13)	C20	C22	C21	C19	-1.1(15)
N2	C10	C6	C1	-26.3(13)	C20	C18	C15	C13	179.5(11)
N2	C10	C6	C5	156.1(9)	C16	C4	C3	C2	177.7(9)
C1	C6	C5	C4	2.1(14)	C16	C4	C3	C13	-3.9(15)
C1	C6	C5	C14	-176.5(10)	C16	C4	C5	C6	-179.1(9)
C1	C2	C7	N1	-33.6(14)	C16	C4	C5	C14	-0.5(14)
C12	N2	C10	C6	161.8(8)	C16	C18	C15	C13	-1.1(16)
C9	N1	C7	C2	164.8(9)	C16	C19	C17	C14	-0.7(16)
C11	N2	C10	C6	-78.4(10)	C3	C4	C16	C18	2.4(15)
C22	C21	C19	C16	-0.4(15)	C3	C4	C16	C19	-177.2(9)
C22	C21	C19	C17	-179.0(10)	C3	C4	C5	C6	-1.1(15)
C22	C20	C18	C16	-0.6(16)	C3	C4	C5	C14	177.6(10)
C22	C20	C18	C15	178.7(10)	C3	C2	C7	N1	146.7(10)
C23	C22	C21	C19	177.2(9)	C18	C16	C19	C21	1.4(15)
C23	C22	C20	C18	-176.5(10)	C18	C16	C19	C17	-179.9(9)
C10	C6	C5	C4	179.6(9)	C18	C15	C13	C3	-0.4(18)
C10	C6	C5	C14	1.1(16)	C19	C16	C18	C20	-1.0(15)
C4	C16	C18	C20	179.5(9)	C19	C16	C18	C15	179.7(10)
C4	C16	C18	C15	0.1(15)	C5	C4	C16	C18	-179.5(9)
C4	C16	C19	C21	-179.0(9)	C5	C4	C16	C19	0.9(15)
C4	C16	C19	C17	-0.4(15)	C5	C4	C3	C2	-0.3(15)
C4	C3	C2	C1	0.8(16)	C5	C4	C3	C13	178.1(10)
C4	C3	C2	C7	-179.5(10)	C5	C14	C17	C19	1.1(17)
C4	C3	C13	C15	2.9(17)	C8	N1	C7	C2	-76.3(11)

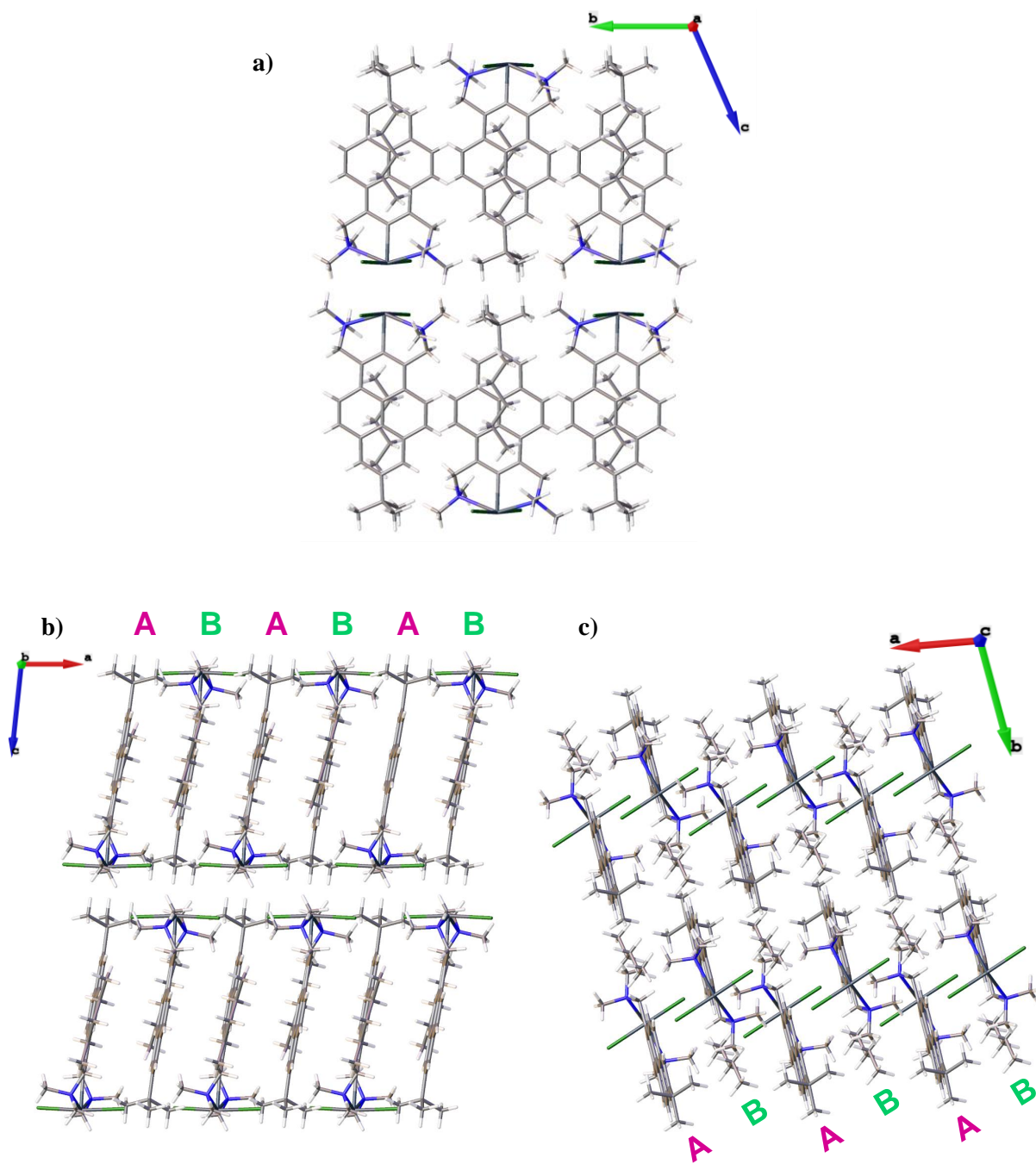


Figure S11. Packing diagrams of complex **1** viewed along (a) the *a*-axis, (b) the *b*-axis, and (c) the *c*-axis of the unit cell.

Table S5. Crystal data and structure refinement for **2**.

Identification code	2
Empirical formula	$C_{45.5}H_{40}BiCl_3N_2$
Formula weight	930.12
Temperature/K	100
Crystal system	monoclinic
Space group	$P2_1/n$
$a/\text{\AA}$	14.0114(6)
$b/\text{\AA}$	20.1875(8)
$c/\text{\AA}$	15.1534(6)
$\alpha/^\circ$	90
$\beta/^\circ$	114.972(3)
$\gamma/^\circ$	90
Volume/ \AA^3	3885.5(3)
Z	4
$\rho_{\text{calc}}/\text{cm}^3$	1.590
μ/mm^{-1}	4.779
$F(000)$	1844.0
Crystal size/ mm^3	$0.25 \times 0.2 \times 0.075$
Radiation	Mo $K\alpha$ ($\lambda = 0.71073$)
2Θ range for data collection/ $^\circ$	5.008 to 50.5
Index ranges	$-16 \leq h \leq 16, -24 \leq k \leq 24, -18 \leq l \leq 18$
Reflections collected	16241
Independent reflections	7021 [$R_{\text{int}} = 0.0453, R_{\text{sigma}} = 0.0569$]
Data/restraints/parameters	7021/36/482
Goodness-of-fit on F^2	1.205
Final R indexes [$I \geq 2\sigma(I)$]	$R_1 = 0.0815, wR_2 = 0.1939$
Final R indexes [all data]	$R_1 = 0.1136, wR_2 = 0.2091$
Largest diff. peak/hole / $e \text{\AA}^{-3}$	1.62/-1.93

Table S6. Bond Lengths [Å] for **2**.

Atom	Atom	Length/Å	Atom	Atom	Length/Å
Bi1	C13	2.334(14)	C24	C23	1.45(2)
Bi1	N2	2.793(14)	C2	C1	1.40(2)
Bi1	C29	2.275(16)	C2	C7	1.52(2)
Bi1	C1	2.270(14)	C2	C3	1.39(2)
C14	C46	1.73(2)	C34	C35	1.37(2)
C13	C46	1.78(2)	C34	C33	1.40(3)
C11	C45	1.77(4)	C19	C18	1.42(2)
N1	C8	1.45(2)	C19	C20	1.42(3)
N1	C9	1.44(2)	C14	C15	1.42(2)
N1	C7	1.49(2)	C25	C26	1.48(2)
C12	C45	1.75(4)	C40	C41	1.35(2)
C13	C14	1.34(2)	C40	C39	1.45(2)
C13	C26	1.43(2)	C43	C44	1.44(2)
N2	C10	1.50(2)	C22	C23	1.36(2)
N2	C12	1.45(2)	C22	C21	1.42(2)
N2	C11	1.45(3)	C1	C6	1.41(2)
C42	C29	1.43(2)	C10	C6	1.53(2)
C42	C43	1.41(2)	C18	C17	1.33(2)
C42	C41	1.44(2)	C6	C5	1.37(2)
C28	C27	1.40(2)	C4	C5	1.38(2)
C28	C19	1.43(2)	C4	C3	1.36(2)
C28	C23	1.44(2)	C35	C36	1.42(2)
C27	C26	1.38(2)	C35	C44	1.44(2)
C27	C16	1.42(2)	C36	C37	1.37(3)
C29	C30	1.39(2)	C15	C16	1.39(2)
C32	C31	1.46(2)	C39	C44	1.44(2)
C32	C43	1.38(2)	C39	C38	1.33(2)
C32	C33	1.41(2)	C17	C16	1.44(2)
C31	C30	1.33(2)	C38	C37	1.36(2)
C24	C25	1.34(2)	C21	C20	1.38(3)

Table S7 Bond Angles [°] for **2**.

Atom	Atom	Atom	Angle/°	Atom	Atom	Atom	Angle/°
C13	Bi1	N2	154.1(5)	C42	C43	C44	119.4(15)
C29	Bi1	C13	82.7(5)	C32	C43	C42	121.7(16)
C29	Bi1	N2	77.1(5)	C32	C43	C44	118.9(15)
C1	Bi1	C13	96.9(5)	C23	C22	C21	119.9(18)
C1	Bi1	N2	69.3(5)	C2	C1	Bi1	120.8(11)
C1	Bi1	C29	95.2(6)	C2	C1	C6	118.3(14)
C8	N1	C7	109.9(14)	C6	C1	Bi1	120.5(11)
C9	N1	C8	108.9(14)	C40	C41	C42	123.1(15)
C9	N1	C7	111.1(13)	N2	C10	C6	111.6(14)
C14	C13	Bi1	121.4(11)	C17	C18	C19	120.5(16)
C14	C13	C26	118.2(14)	C1	C6	C10	120.9(14)
C26	C13	Bi1	120.4(10)	C5	C6	C1	120.1(15)
C10	N2	Bi1	100.5(10)	C5	C6	C10	119.1(15)
C12	N2	Bi1	116.5(11)	C3	C4	C5	119.5(16)
C12	N2	C10	110.8(15)	C34	C35	C36	121.1(16)
C11	N2	Bi1	103.8(10)	C34	C35	C44	120.3(16)
C11	N2	C10	110.9(15)	C36	C35	C44	118.6(16)
C11	N2	C12	113.4(16)	C37	C36	C35	118.7(16)
C29	C42	C41	121.2(14)	C28	C23	C24	115.0(15)
C43	C42	C29	121.0(15)	C22	C23	C28	122.4(17)
C43	C42	C41	117.8(14)	C22	C23	C24	122.5(16)
C27	C28	C19	121.4(15)	C13	C26	C25	121.2(13)
C27	C28	C23	121.6(15)	C27	C26	C13	120.7(14)
C19	C28	C23	117.0(15)	C27	C26	C25	118.0(15)
C28	C27	C16	118.8(15)	C16	C15	C14	118.3(16)
C26	C27	C28	121.3(15)	C44	C39	C40	115.2(14)
C26	C27	C16	119.8(14)	C38	C39	C40	125.3(17)
C42	C29	Bi1	120.6(11)	C38	C39	C44	119.5(16)
C30	C29	Bi1	124.4(12)	C6	C5	C4	121.0(16)
C30	C29	C42	114.7(14)	C18	C17	C16	123.1(17)
C43	C32	C31	116.8(15)	C43	C44	C39	122.4(15)
C43	C32	C33	120.8(16)	C35	C44	C43	119.1(15)
C33	C32	C31	122.3(16)	C35	C44	C39	118.5(15)
C30	C31	C32	119.4(14)	C34	C33	C32	120.5(17)
C25	C24	C23	124.1(16)	C39	C38	C37	122.2(19)
C1	C2	C7	121.8(14)	C27	C16	C17	118.0(16)
C3	C2	C1	119.2(15)	C15	C16	C27	119.6(15)
C3	C2	C7	118.7(14)	C15	C16	C17	122.3(16)
C35	C34	C33	120.1(16)	C38	C37	C36	122.5(18)
C18	C19	C28	118.2(15)	N1	C7	C2	111.8(13)
C18	C19	C20	122.5(16)	C20	C21	C22	119.9(17)
C20	C19	C28	119.3(16)	C4	C3	C2	121.0(16)

Atom	Atom	Atom	Angle/°	Atom	Atom	Atom	Angle/°
C13	C14	C15	123.3(16)	C21	C20	C19	121.4(17)
C24	C25	C26	119.6(16)	C14	C46	C13	112.7(11)
C31	C30	C29	125.9(15)	C12	C45	C11	111(2)
C41	C40	C39	122.0(16)				

Table S8. Torsion Angles [°] for **2**.

A	B	C	D	Angle/°	A	B	C	D	Angle/°
Bi1	C13	C14	C15	-179.0(12)	C43	C32	C31	C30	-7(2)
Bi1	C13	C26	C27	179.3(11)	C43	C32	C33	C34	-6(2)
Bi1	C13	C26	C25	-3(2)	C22	C21	C20	C19	-1(3)
Bi1	N2	C10	C6	41.8(15)	C1	C2	C7	N1	39(2)
Bi1	C29	C30	C31	-175.1(12)	C1	C2	C3	C4	3(2)
Bi1	C1	C6	C10	-1(2)	C1	C6	C5	C4	3(3)
Bi1	C1	C6	C5	178.4(13)	C41	C42	C29	Bi1	-8.0(19)
C13	C14	C15	C16	-1(3)	C41	C42	C29	C30	178.1(14)
N2	C10	C6	C1	-34(2)	C41	C42	C43	C32	-178.1(14)
N2	C10	C6	C5	146.2(16)	C41	C42	C43	C44	3(2)
C8	N1	C7	C2	64.8(17)	C41	C40	C39	C44	-1(2)
C42	C29	C30	C31	-1(2)	C41	C40	C39	C38	-178.1(16)
C42	C43	C44	C35	176.4(14)	C10	C6	C5	C4	-177.5(16)
C42	C43	C44	C39	-4(2)	C18	C19	C20	C21	-179.4(16)
C28	C27	C26	C13	-174.9(15)	C18	C17	C16	C27	2(3)
C28	C27	C26	C25	7(2)	C18	C17	C16	C15	-178.0(17)
C28	C27	C16	C15	177.5(15)	C35	C34	C33	C32	6(3)
C28	C27	C16	C17	-2(2)	C35	C36	C37	C38	2(3)
C28	C19	C18	C17	-2(2)	C36	C35	C44	C43	178.7(14)
C28	C19	C20	C21	0(3)	C36	C35	C44	C39	-1(2)
C27	C28	C19	C18	1(2)	C23	C28	C27	C26	-4(2)
C27	C28	C19	C20	-178.5(15)	C23	C28	C27	C16	-179.3(15)
C27	C28	C23	C24	0(2)	C23	C28	C19	C18	-178.5(15)
C27	C28	C23	C22	177.1(17)	C23	C28	C19	C20	2(2)
C29	C42	C43	C32	5(2)	C23	C24	C25	C26	3(3)
C29	C42	C43	C44	-174.2(14)	C23	C22	C21	C20	0(3)
C29	C42	C41	C40	175.7(15)	C26	C13	C14	C15	3(2)
C32	C31	C30	C29	7(2)	C26	C27	C16	C15	2(2)
C32	C43	C44	C35	-2(2)	C26	C27	C16	C17	-177.9(15)
C32	C43	C44	C39	177.5(14)	C39	C40	C41	C42	1(2)
C31	C32	C43	C42	1(2)	C39	C38	C37	C36	-4(3)
C31	C32	C43	C44	-180.0(13)	C5	C4	C3	C2	-9(3)
C31	C32	C33	C34	178.5(15)	C44	C35	C36	C37	0(2)

A	B	C	D	Angle/°	A	B	C	D	Angle/°
C24	C25	C26	C13	175.6(15)	C44	C39	C38	C37	3(2)
C24	C25	C26	C27	-7(2)	C33	C32	C31	C30	168.3(15)
C2	C1	C6	C10	172.0(15)	C33	C32	C43	C42	-174.1(15)
C2	C1	C6	C5	-8(2)	C33	C32	C43	C44	5(2)
C34	C35	C36	C37	177.2(16)	C33	C34	C35	C36	179.7(16)
C34	C35	C44	C43	2(2)	C33	C34	C35	C44	-3(2)
C34	C35	C44	C39	-178.1(14)	C38	C39	C44	C43	179.9(15)
C19	C28	C27	C26	176.3(15)	C38	C39	C44	C35	0(2)
C19	C28	C27	C16	1(2)	C12	N2	C10	C6	165.6(15)
C19	C28	C23	C24	179.5(14)	C16	C27	C26	C13	0(2)
C19	C28	C23	C22	-3(2)	C16	C27	C26	C25	-177.4(14)
C19	C18	C17	C16	0(3)	C9	N1	C7	C2	-174.6(13)
C14	C13	C26	C27	-3(2)	C7	C2	C1	Bi1	3.8(19)
C14	C13	C26	C25	174.6(15)	C7	C2	C1	C6	-169.4(14)
C14	C15	C16	C27	-2(2)	C7	C2	C3	C4	178.3(15)
C14	C15	C16	C17	178.2(16)	C21	C22	C23	C28	2(3)
C25	C24	C23	C28	1(3)	C21	C22	C23	C24	179.6(17)
C25	C24	C23	C22	-176.5(18)	C11	N2	C10	C6	-67.5(18)
C40	C39	C44	C43	2(2)	C3	C2	C1	Bi1	178.4(11)
C40	C39	C44	C35	-177.8(13)	C3	C2	C1	C6	5(2)
C40	C39	C38	C37	179.8(16)	C3	C2	C7	N1	-136.1(14)
C43	C42	C29	Bi1	169.4(11)	C3	C4	C5	C6	6(3)
C43	C42	C29	C30	-5(2)	C20	C19	C18	C17	177.9(17)
C43	C42	C41	C40	-2(2)					

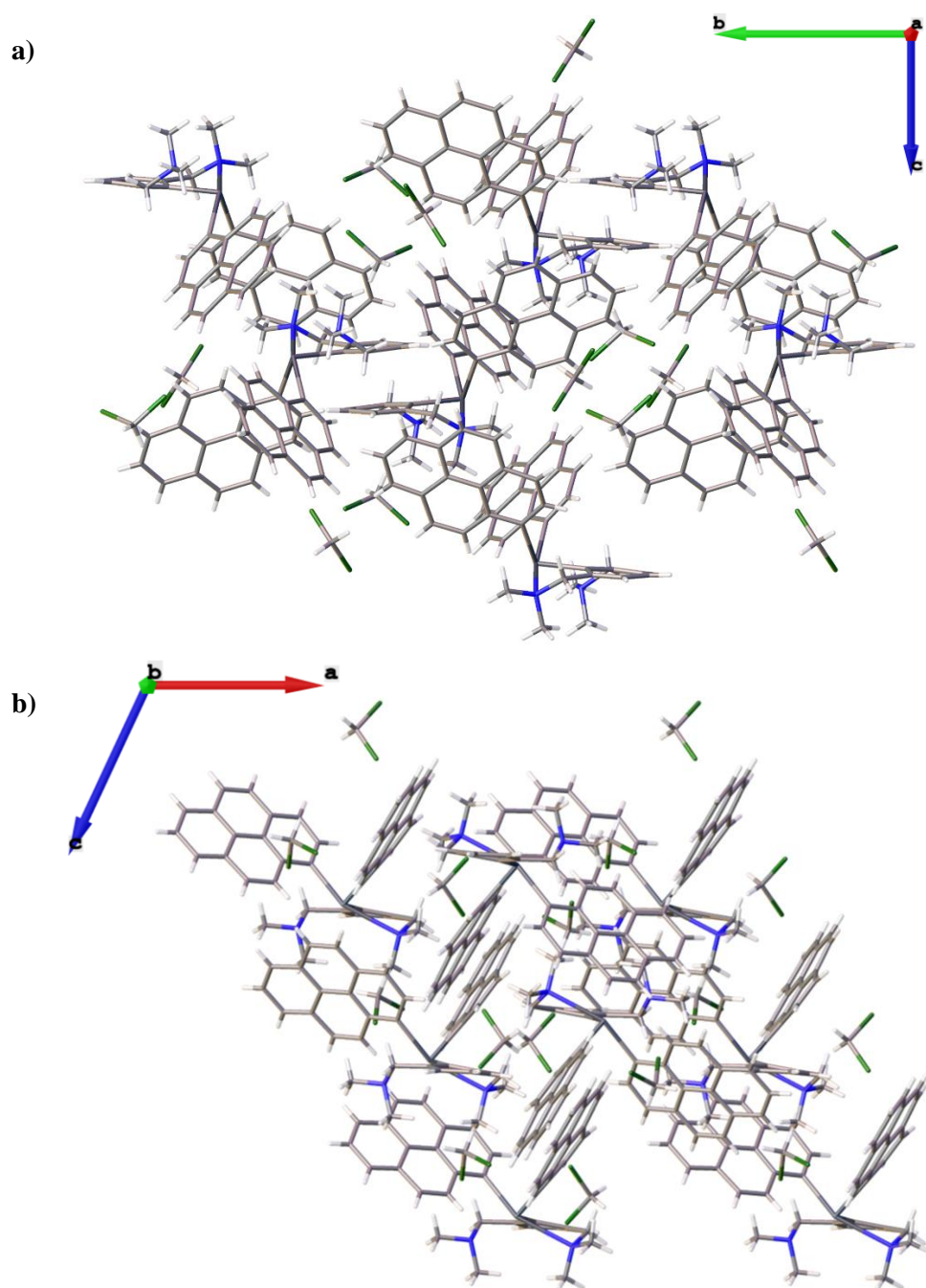


Figure S12. Packing diagrams of complex **2** viewed along (a) the *a*-axis and (b) the *b*-axis of the unit cell.

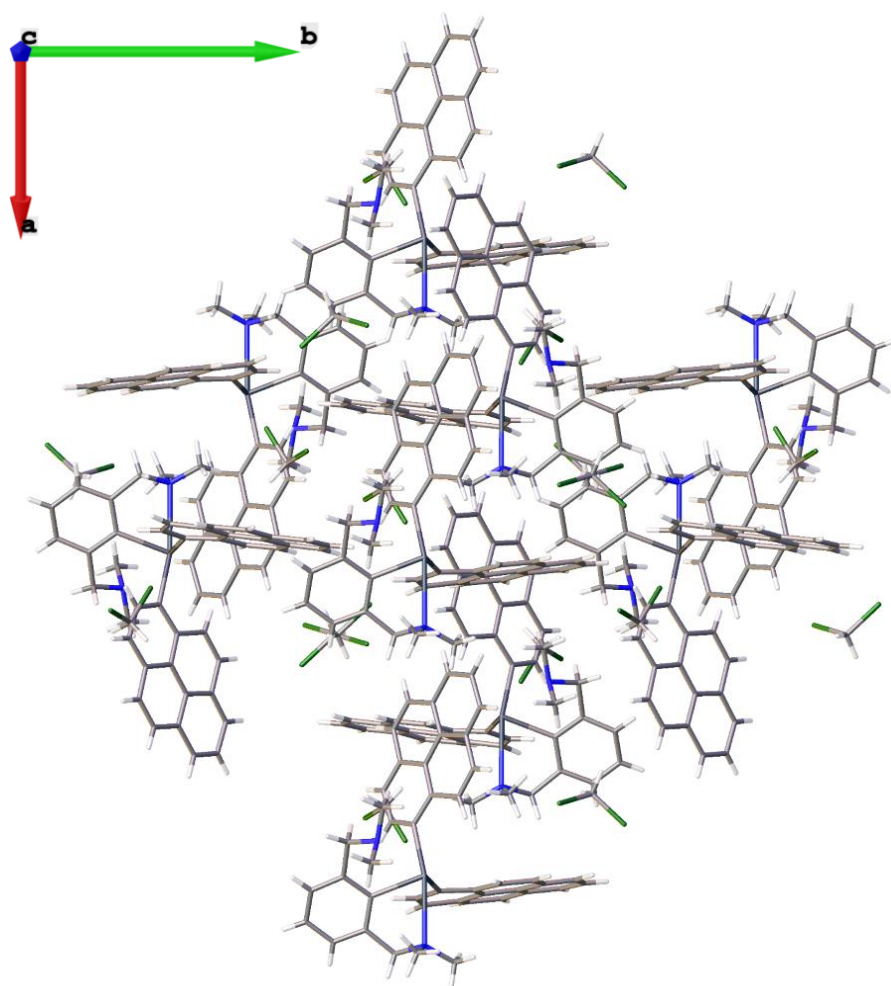


Figure S13. Packing diagrams of complex **2** viewed along the *c*-axis of the unit cell.

UV/Vis Spectroscopy

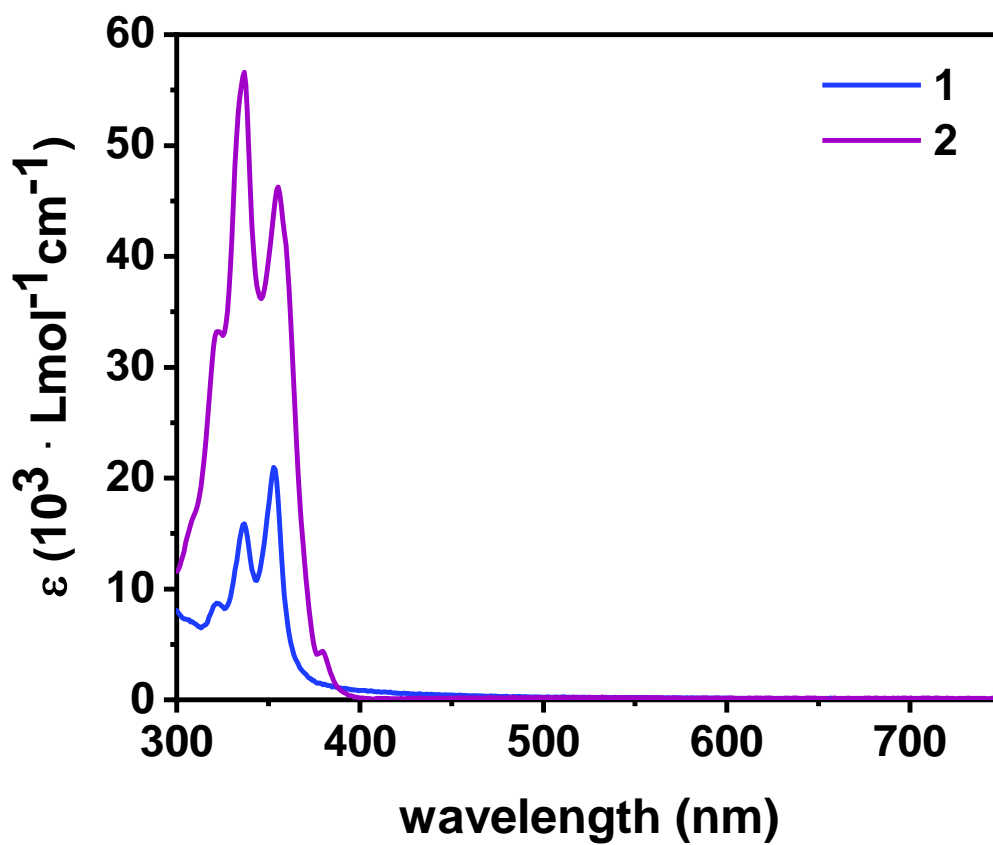


Figure S14. UV/Vis absorption spectra of **1** (top) and **2** (bottom) in CH₂Cl₂.

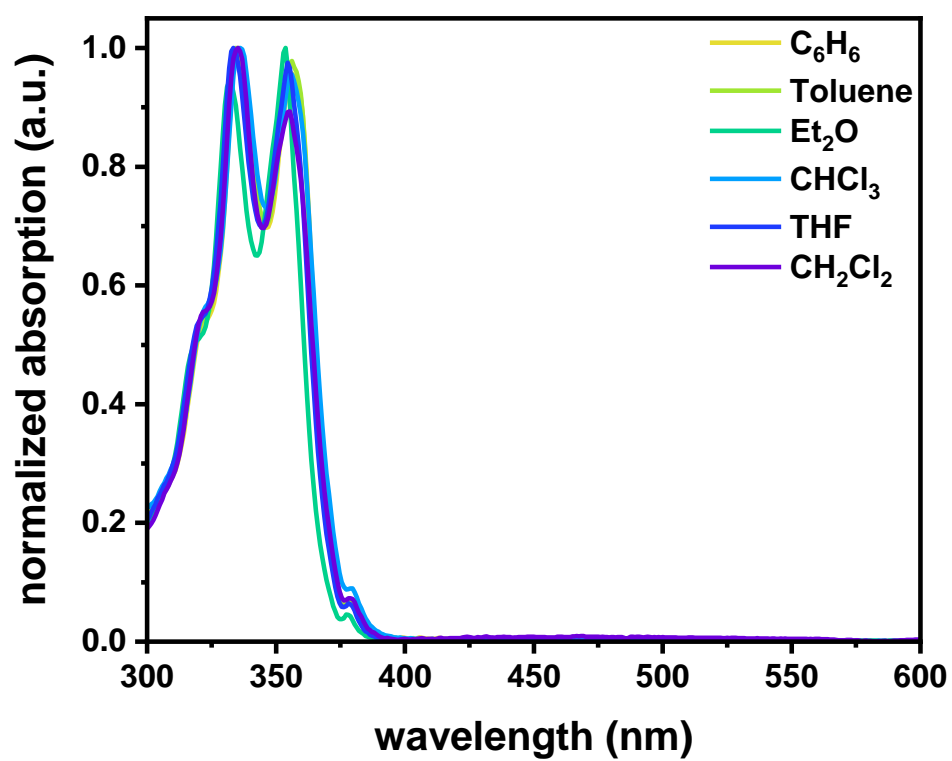
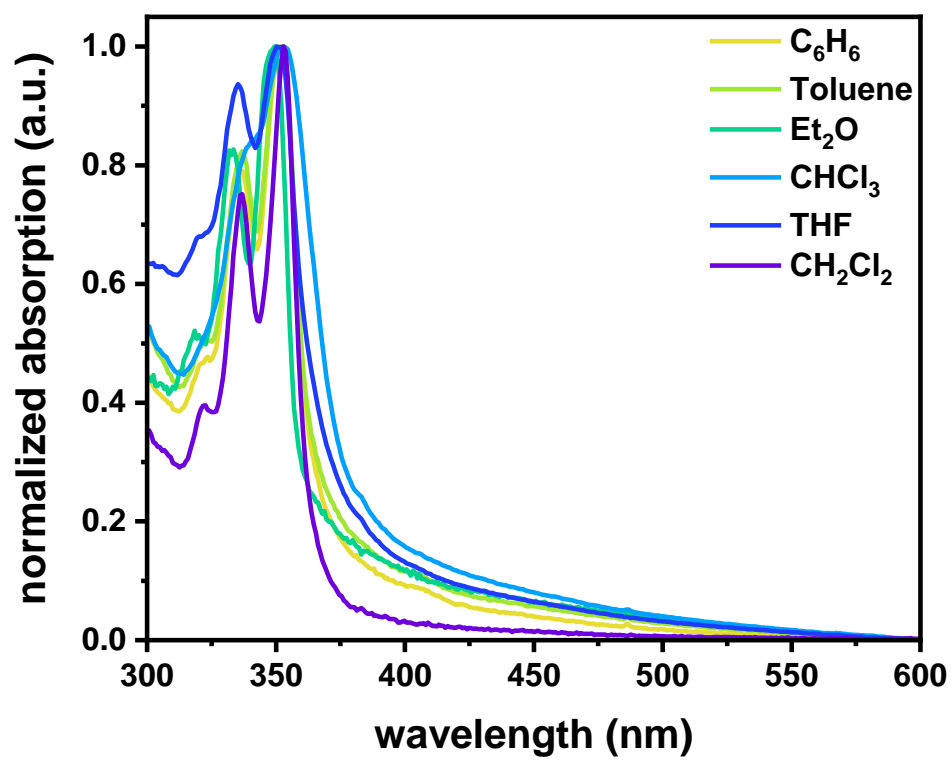


Figure S15. UV/Vis absorption spectra of 1 (top) and 2 (bottom) in different solvents.

TD-DFT Data

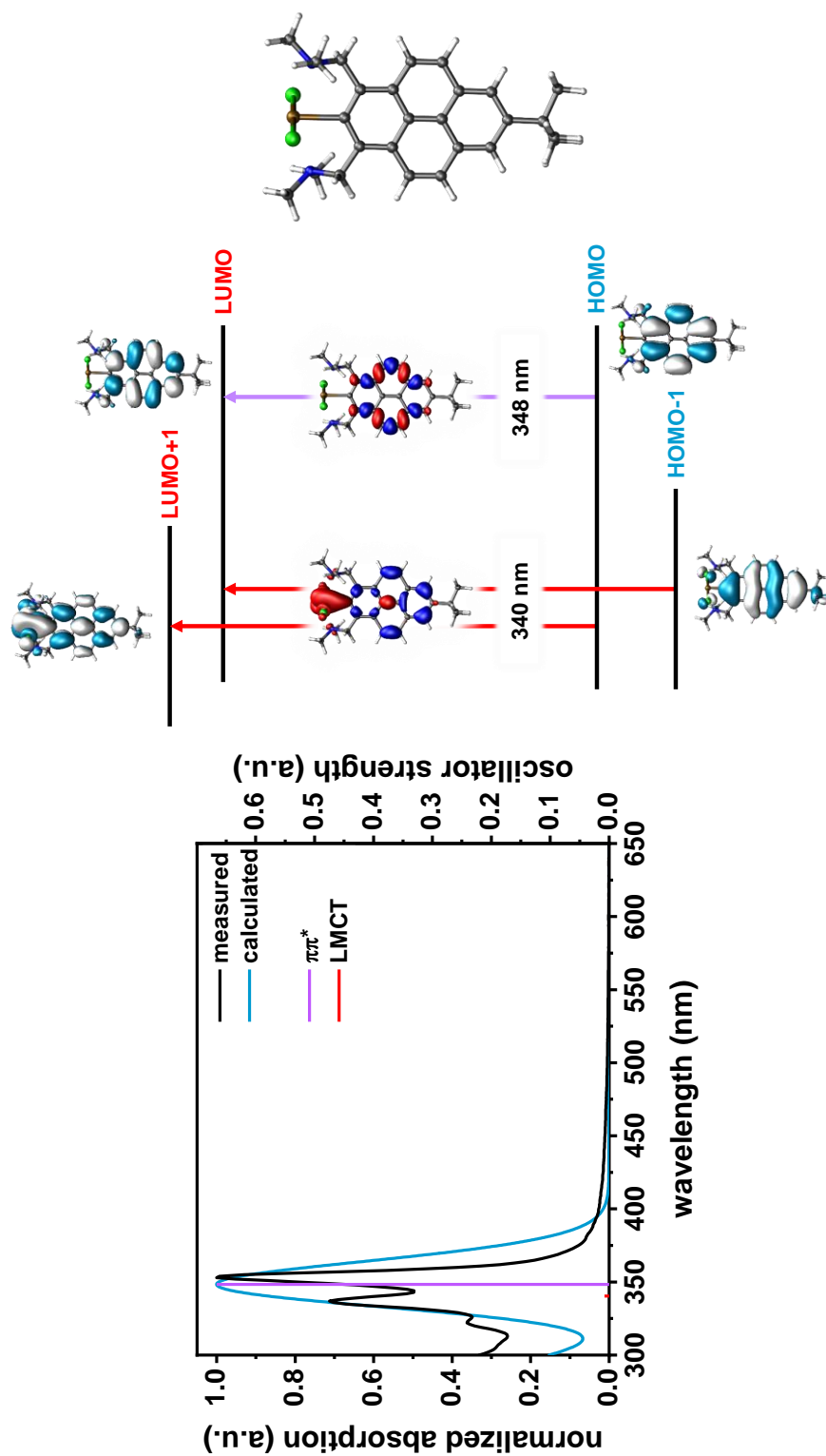


Figure S16. Top: Geometry-optimized structure of complex **1**. Middle: MO diagrams of relevant molecular orbitals involved in the individual TD-DFT computed electronic transitions along with the corresponding electron density difference maps. A loss of electron density is indicated in blue, a gain in red colour. Bottom: Comparison between the experimental (black line) and the TD-DFT computed (blue line) electronic absorption spectra. Individual electronic transitions are indicated as coloured bars.

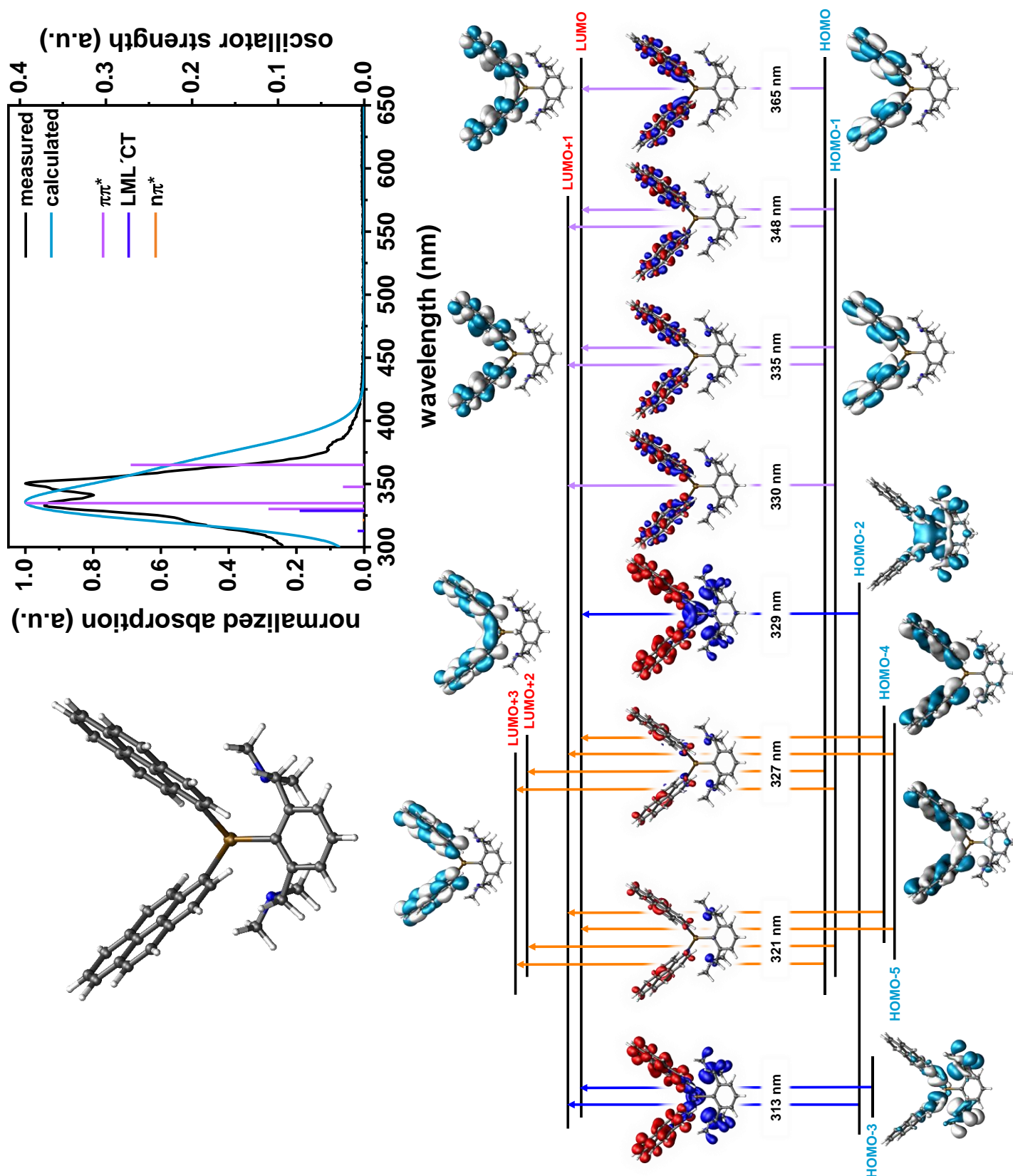


Figure S17. Left: Geometry-optimized structure of complex 2 along with comparison between the experimental (black line) and the TD-DFT computed (blue line) electronic absorption spectra. Individual electronic transitions are indicated as coloured bars. Right: MO diagrams of relevant molecular orbitals involved in the individual TD-DFT computed electronic transitions along with the corresponding electron density difference maps. A loss of electron density is indicated in blue, a gain in red colour.

Table S9. XYZ coordinates of the DFT-optimized structure of complex **1**.

Atom	X	Y	Z
Bi	-3.20610	-0.00533	0.00033
C	-0.99396	0.00312	0.00026
N	-2.45052	2.36191	0.48413
C	-3.41620	3.35122	-0.00935
H	-3.61380	3.17051	-1.06884
H	-3.03058	4.37225	0.12054
H	-4.34965	3.25588	0.55196
N	-2.43252	-2.36638	-0.48457
C	-2.23104	2.54382	1.92571
H	-3.16830	2.38953	2.46455
H	-1.85963	3.55888	2.12748
H	-1.50097	1.81481	2.28289
C	-1.17142	2.47309	-0.24382
H	-0.64555	3.37066	0.10654
H	-1.41094	2.62231	-1.30357
C	-2.21066	-2.54623	-1.92600
H	-3.14858	-2.39831	-2.46547
H	-1.83193	-3.55859	-2.12777
H	-1.48545	-1.81203	-2.28242
C	-1.15325	-2.46839	0.24452
H	-1.39288	-2.61788	1.30421
H	-0.62132	-3.36295	-0.10434
C	-3.39151	-3.36274	0.00774
H	-3.59098	-3.18415	1.06724
H	-2.99873	-4.38097	-0.12262
H	-4.32529	-3.27350	-0.55406
Cl	-3.19769	-0.75599	2.59053
Cl	-3.20358	0.74516	-2.58979
C	6.06244	0.03149	-0.00231
C	5.33606	1.21564	-0.13150
C	3.93364	1.23408	-0.13267
C	3.21153	0.01841	-0.00127
C	3.94377	-1.19417	0.12988
C	5.34122	-1.16157	0.12755
C	3.19659	2.45280	-0.26590
C	1.78562	0.01300	-0.00080
C	1.07751	1.24889	-0.11766
C	1.83748	2.45928	-0.25870
C	-0.33219	1.22446	-0.09592
C	-0.32229	-1.21426	0.09589
C	1.08633	-1.22818	0.11641
C	1.85594	-2.43406	0.25691
C	3.21406	-2.41888	0.26346
H	3.77100	-3.34643	0.37205
H	1.34215	-3.38269	0.37092
H	3.74716	3.38412	-0.37483
H	5.85152	2.16547	-0.23537
H	5.87012	-2.10628	0.23092
H	1.31737	3.40448	-0.37254
C	7.59261	-0.00338	0.00052
C	8.08530	-0.61221	1.32366
C	8.08238	-0.86850	-1.17243
C	8.20662	1.39168	-0.14307
H	7.75419	-0.01139	2.17840
H	7.71639	-1.63361	1.46561
H	9.18130	-0.64817	1.33614
H	7.75212	-0.45175	-2.13079
H	9.17826	-0.90984	-1.17790
H	7.70951	-1.89606	-1.10458
H	9.29931	1.31130	-0.13419
H	7.91758	1.86972	-1.08615
H	7.91636	2.05201	0.68230

Table S10. XYZ coordinates of the DFT-optimized structure of complex **2**.

Atom	X	Y	Z
Bi	0.00450	-1.29574	-0.74442
N	-2.49407	-2.90117	-0.98931
C	-1.54562	-0.09393	0.47048
N	2.50498	-2.88163	-1.02409
C	-2.25595	-4.04321	-1.85690
H	-3.06627	-4.79222	-1.79191
H	-1.31561	-4.53164	-1.58573
H	-2.18313	-3.70390	-2.89527
C	2.28091	0.96577	-0.13923
C	-3.93040	2.79769	0.05465
C	-3.17669	1.74586	0.65392
C	1.55598	-0.08751	0.46175
C	3.32649	1.50151	2.03573
C	2.60019	0.44885	2.60447
H	2.71645	0.23622	3.66537
C	-2.92679	2.24132	-2.11326
H	-2.84071	2.43641	-3.17973
C	-1.18985	-3.78019	0.91351
C	4.91818	3.33223	2.23726
H	5.59244	3.94222	2.83377
C	-4.80913	3.59304	0.84714
C	-1.70400	-0.30795	1.84387
H	-1.14537	-1.10472	2.33104
C	-2.21016	1.23928	-1.53921
H	-1.55647	0.63173	-2.16079
C	1.73625	-0.31753	1.82984
H	1.19384	-1.12720	2.31410
C	2.87350	2.29738	-2.10989
H	2.76927	2.50612	-3.17214
C	3.16940	1.76754	0.64634
C	-4.56003	4.09909	-1.90954
H	-4.46579	4.29642	-2.97473
C	0.01785	-3.15012	0.55701
C	2.17600	1.28008	-1.53911
H	1.51906	0.67460	-2.15926
C	2.56407	-3.27262	0.37924
H	2.88278	-2.39133	0.94800
H	3.33107	-4.05281	0.54300
C	-4.91891	3.31319	2.24925
H	-5.59091	3.92405	2.84743
C	1.23396	-3.77442	0.89485
C	0.03552	-5.48489	2.12720
H	0.04240	-6.37873	2.74533
C	4.78514	3.62926	0.84071
C	5.49502	4.67352	0.23252
H	6.16650	5.27817	0.83753
C	-3.81155	3.06049	-1.33971
C	-2.29089	0.94319	-0.13373
C	-2.56545	0.45908	2.62063
H	-2.66444	0.25921	3.68575
C	3.76123	3.11525	-1.33840
C	1.22980	-4.92534	1.68942
H	2.17627	-5.39753	1.94530
C	-4.20276	2.31038	2.82201
H	-4.29318	2.10664	3.88652
C	3.90324	2.83520	0.05041
C	4.22079	2.31454	2.80688
H	4.32870	2.09780	3.86718
C	4.49051	4.16916	-1.90504
H	4.37863	4.37963	-2.96600
C	3.71988	-2.19052	-1.42159
H	3.62779	-1.85463	-2.45959
H	4.61268	-2.83781	-1.34691
H	3.87046	-1.31262	-0.78738
C	-3.31106	1.49650	2.04875

C	5.34747	4.93888	-1.12516
H	5.90570	5.75303	-1.57940
C	-3.72087	-2.22241	-1.37143
H	-3.64789	-1.89093	-2.41235
H	-3.86932	-1.34269	-0.73928
H	-4.60672	-2.87705	-1.27967
C	-2.52965	-3.28550	0.41680
H	-3.29107	-4.06773	0.59613
H	-2.84278	-2.40260	0.98615
C	-5.41358	4.87038	-1.12745
H	-5.98681	5.67260	-1.58424
C	2.26193	-4.02079	-1.89404
H	1.32974	-4.51787	-1.61069
H	3.07887	-4.76381	-1.84593
H	2.16996	-3.67652	-2.92926
C	-1.16803	-4.93091	1.70804
H	-2.10821	-5.40754	1.97847
C	-5.53867	4.62173	0.23562
H	-6.20759	5.22751	0.84233

Photoluminescence Data

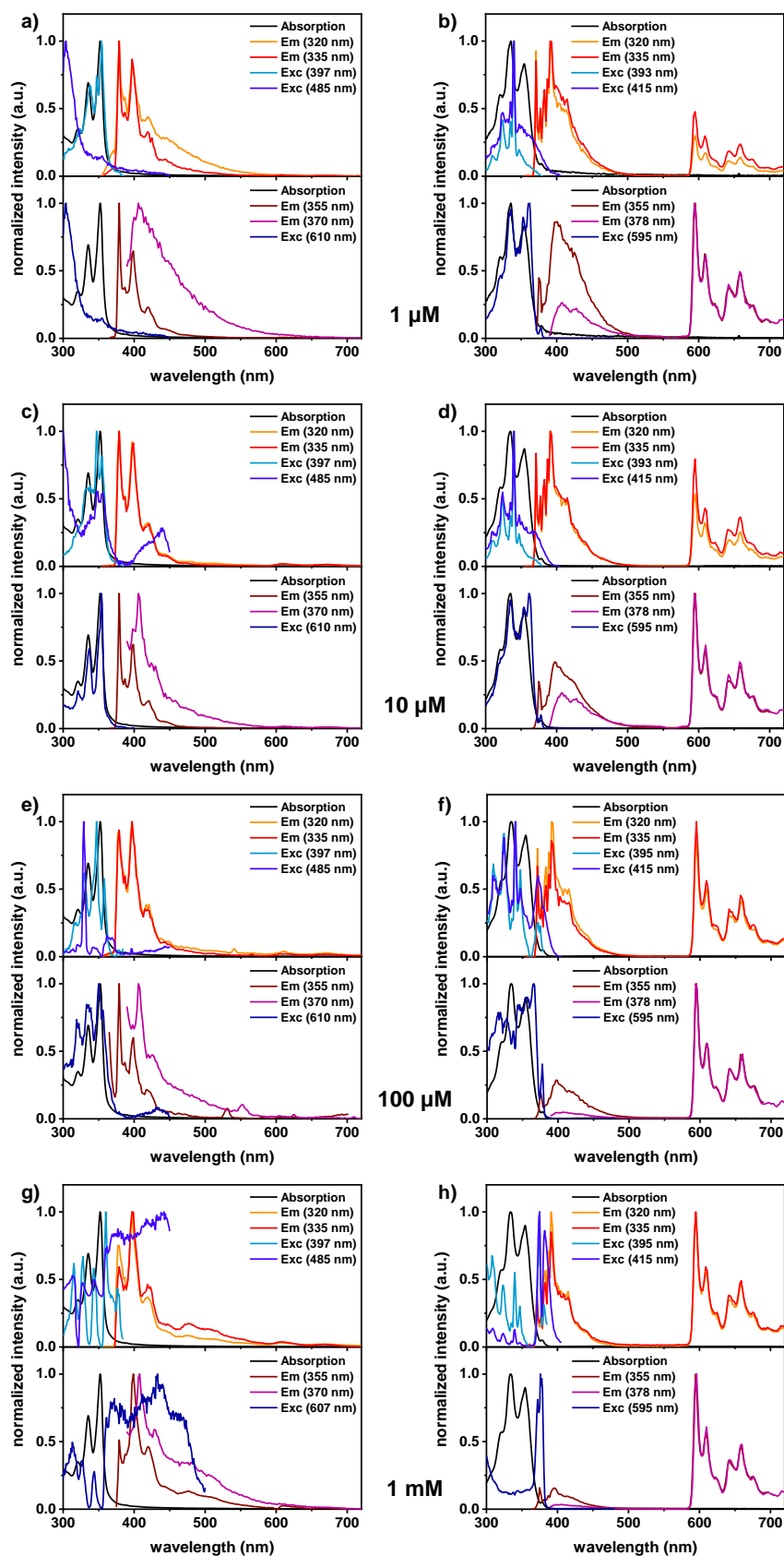


Figure S18. PL data at 77 K in MeTHF of (a) **1** at $c = 1 \mu\text{M}$. (b) **2** at $c = 1 \mu\text{M}$. (c) **1** at $c = 10 \mu\text{M}$. (d) **2** at $c = 10 \mu\text{M}$. (e) **1** at $c = 100 \mu\text{M}$. (f) **2** at $c = 100 \mu\text{M}$. (g) **1** at $c = 1 \text{mM}$. (h) **2** at $c = 1 \text{mM}$. Absorption spectra are depicted as black, emission spectra as red and excitation spectra as blue lines.

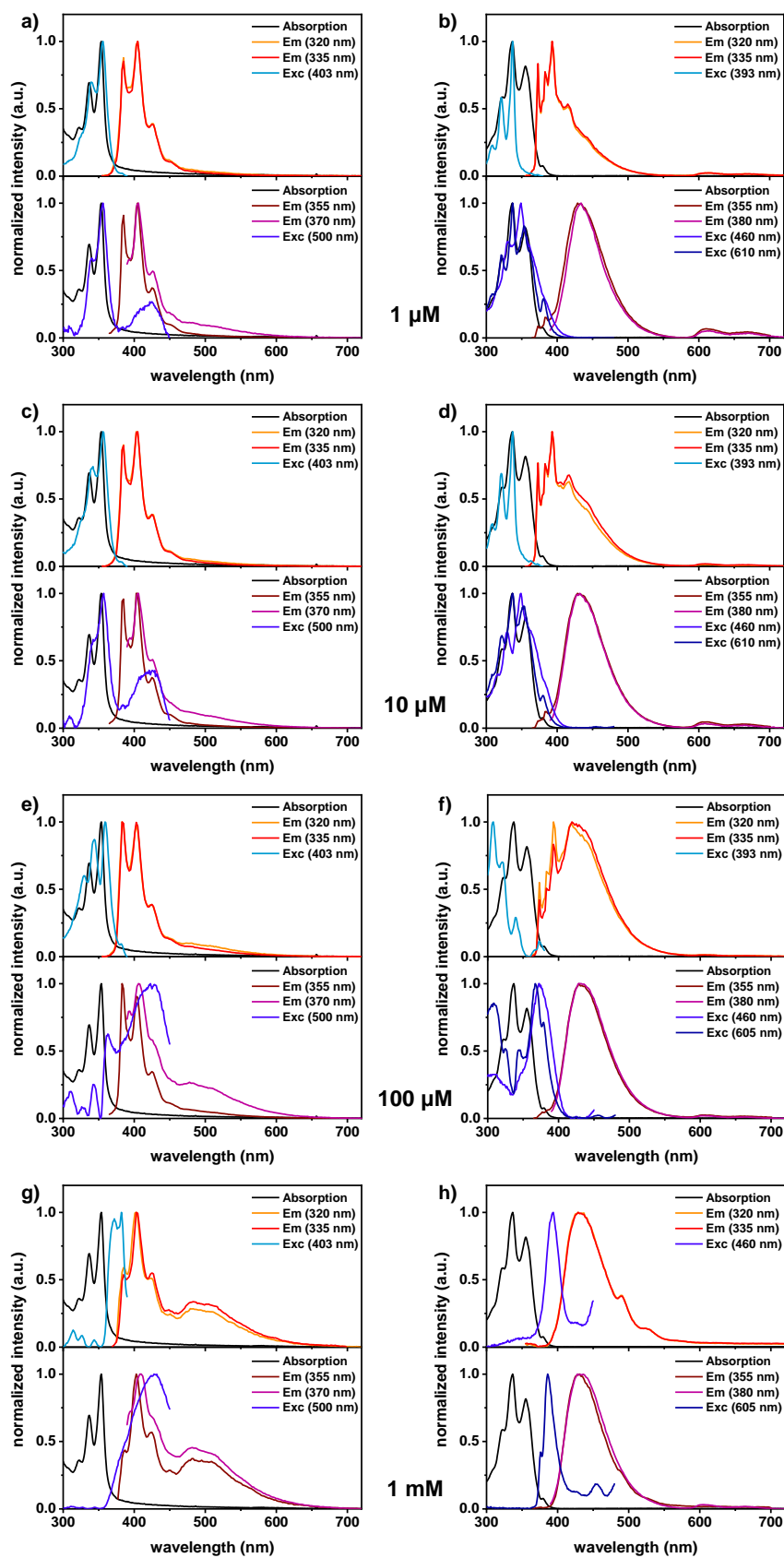


Figure S19. PL data at r.t. in degassed CH_2Cl_2 of (a) **1** at $c = 1 \mu\text{M}$. (b) **2** at $c = 1 \mu\text{M}$. (c) **1** at $c = 10 \mu\text{M}$. (d) **2** at $c = 10 \mu\text{M}$. (e) **1** at $c = 100 \mu\text{M}$. (f) **2** at $c = 100 \mu\text{M}$. (g) **1** at $c = 1 \text{mM}$. (h) **2** at $c = 1 \text{mM}$. Absorption spectra are depicted as black, emission spectra as red and excitation spectra as blue lines.

Table S11. Photoluminescence and absorption data for complexes **1** and **2**.

	λ_{\max} (nm), [$\epsilon\lambda$] ($\times 10^{-3} \cdot \text{M}^{-1} \text{cm}^{-1}$) ^b	λ_{Em} (nm)	λ_{Exc} (nm)	τ_{F} (ns) ^c	τ_{P} (ms) ^c
1	322 [8.4] 337 [15.8] 354 [20.9]	F : 379, 387, 397, 421 ^a ^aP : 610, 675 ^a	335, 347, 354 ^a 321, 337, 354 ^a	20 [40%], 170 [60%] ^a -	- 2.0 [97%], 10 [3%] ^a
		F : 385, 405, 425, 451 ^b	326, 341, 356 ^b	17 [15%], 59 [85%] ^b	-
2	322 [31.6] 337 [56.6] 355 [50.6] 380 [4.5]	F : 371, 377, 383, 387, 391, 415 ^a P : 595, 610, 642, 658 ^a	310, 323, 335, 340, 347 ^a 321, 335, 354, 361, 378 ^a	2.3 [95%], 13 [4%], 150 [1%] ^a -	- 4.6 [100%] ^a
		F : 373, 383, 393, 417 ^b ^bExcimer : 432 ^b	308, 321, 337, 363 ^b 394 ^b	2.5 [84%], 20 [13%], 132 [3%] ^b 2.5 [100%]	- -
		^bP : 610, 665 ^b	322, 337, 353, 380 ^b	-	0.10 [58%], 0.21 [42%] ^b

^a In MeTHF at 77 K; ^b in CH₂Cl₂ at r.t., ^c relative contributions in [%].

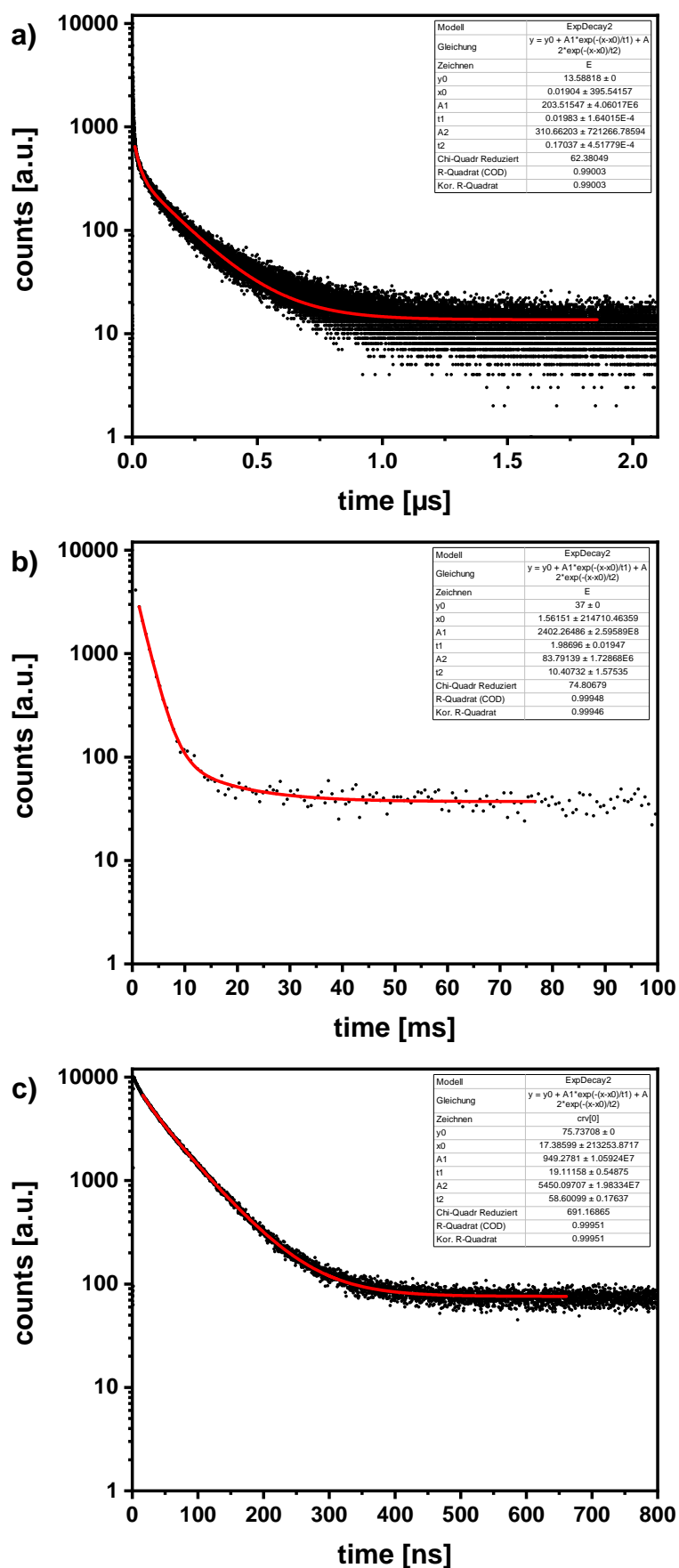


Figure S20. Lifetime measurements of (a) the 397 nm emission of **1** at 77 K in MeTHF; (b) the 610 nm emission of **1** at 77 K in MeTHF; (c) the 403 nm emission of **1** in degassed CH₂Cl₂ at r.t..

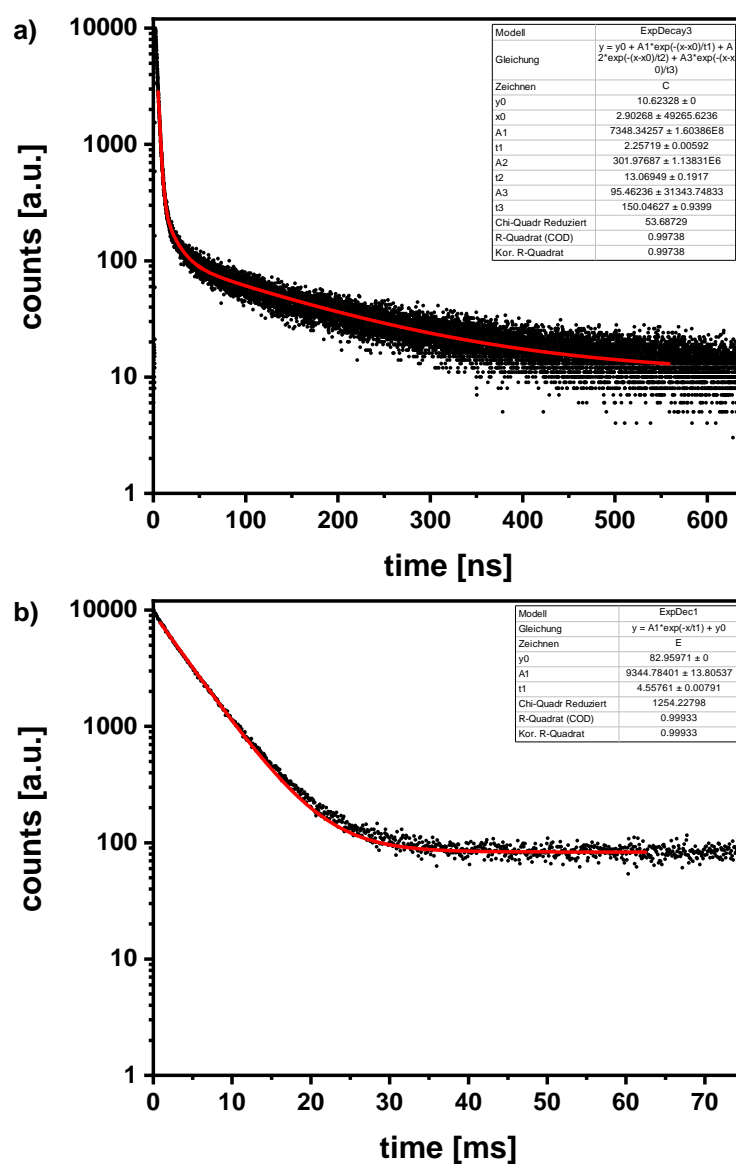


Figure S21. Lifetime measurements of (a) the 393 nm emission of **2** at 77 K in MeTHF; (b) the 595 nm emission of **2** at 77 K in MeTHF.

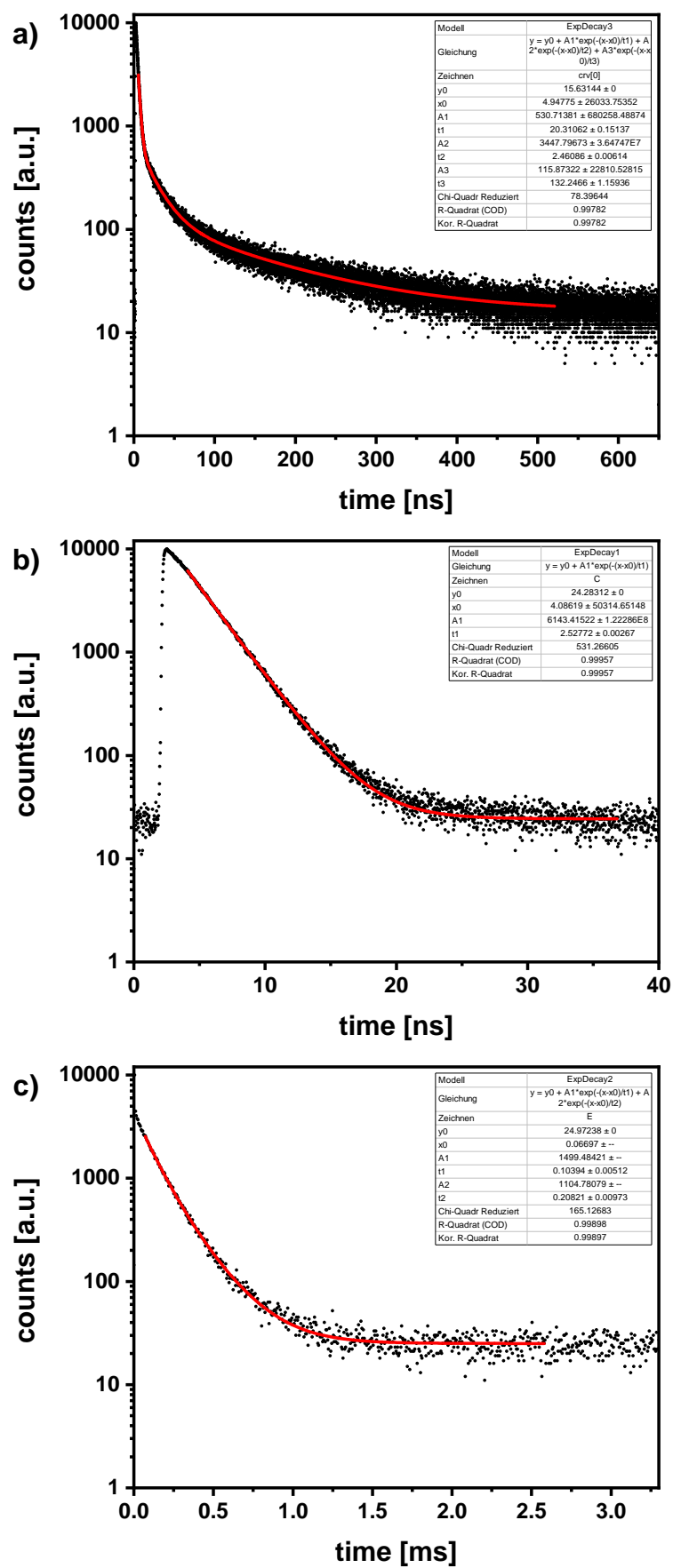


Figure S22. Lifetime measurements of (a) the 393 nm emission of **2** at r.t. in degassed CH₂Cl₂; (b) the 430 nm emission of **2** at r.t. in degassed CH₂Cl₂; (c) the 610 nm emission of **2** at r.t. in degassed CH₂Cl₂.

References

1. H. Maeda, M. Hironishi, R. Ishibashi, K. Mizuno and M. Segi, *Photochem. Photobiol. Sci.*, 2017, **16**, 228-237.
2. C. S. Albert P. Soran, Hans J. Breunig, Gabor Balázs, Jennifer C. Green, *Organometallics*, 2007, **26**, 1196-1203.
3. D. Kratzert, J. J. Holstein and I. Krossing, *J. Appl. Crystallogr.*, 2015, **48**, 933-938.
4. G. Sheldrick, *Acta Crystallogr. A*, 2015, **71**, 3-8.
5. O. V. Dolomanov, L. J. Bourhis, R. J. Gildea, J. A. K. Howard and H. Puschmann, *J. Appl. Crystallogr.*, 2009, **42**, 339-341.
6. M. J. Frisch, G. W. Trucks, H. B. Schlegel, G. E. Scuseria, M. A. Robb, J. R. Cheeseman, G. Scalmani, V. Barone, G. A. Petersson, H. Nakatsuji, X. Li, M. Caricato, A. V. Marenich, J. Bloino, B. G. Janesko, R. Gomperts, B. Mennucci, H. P. Hratchian, J. V. Ortiz, A. F. Izmaylov, J. L. Sonnenberg, Williams, F. Ding, F. Lipparini, F. Egidi, J. Goings, B. Peng, A. Petrone, T. Henderson, D. Ranasinghe, V. G. Zakrzewski, J. Gao, N. Rega, G. Zheng, W. Liang, M. Hada, M. Ehara, K. Toyota, R. Fukuda, J. Hasegawa, M. Ishida, T. Nakajima, Y. Honda, O. Kitao, H. Nakai, T. Vreven, K. Throssell, J. A. Montgomery Jr., J. E. Peralta, F. Ogliaro, M. J. Bearpark, J. J. Heyd, E. N. Brothers, K. N. Kudin, V. N. Staroverov, T. A. Keith, R. Kobayashi, J. Normand, K. Raghavachari, A. P. Rendell, J. C. Burant, S. S. Iyengar, J. Tomasi, M. Cossi, J. M. Millam, M. Klene, C. Adamo, R. Cammi, J. W. Ochterski, R. L. Martin, K. Morokuma, O. Farkas, J. B. Foresman and D. J. Fox, *Wallingford, CT*, 2016.
7. A. V. Marenich, C. J. Cramer and D. G. Truhlar, *J. Phys. Chem. B*, 2009, **113**, 6378-6396.
8. B. Metz, H. Stoll and M. Dolg, *J. Chem. Phys.*, 2000, **113**, 2563-2569.
9. P. C. Hariharan and J. A. Pople, *Theor. Chim. Acta*, 1973, **28**, 213-222.
10. J. P. Perdew, K. Burke and M. Ernzerhof, *Phys. Rev. Lett.*, 1996, **77**, 3865-3868.
11. C. Adamo and V. Barone, *J. Phys. Chem.*, 1999, **110**, 6158-6170.
12. N. M. O'Boyle, A. L. Tenderholt and K. M. Langner, *J. Comp. Chem.*, 2008, **29**, 839-845.
13. M. D. Hanwell, D. E. Curtis, D. C. Lonie, T. Vandermeersch, E. Zurek and G. R. Hutchison, *J. Cheminformatics*, 2012, **4**, 17.
14. O. Tange, *login: The USENIX Magazine*, 2011, **36**, 42-47.
15. W. Humphrey, A. Dalke and K. Schulten, *J. Mol. Graph.*, 1996, **14**, 33-38.
16. Povray.org, <http://www.povray.org/download/>, (accessed 29.01.2024).